REPORT METEOROLOGY AND CLIMATOLOGY No. 124, 2026

Long-term (1990-2023) reanalysis of phytotoxic ozone dose (PODY) for Sweden

Magnuz Engardt and Camilla Andersson

Front:
Spruce forest potentially impacted by exposure to near-surface ozone.

ISSN: 0347-2116 © SMHI

REPORT METEOROLOGY AND CLIMATOLOGY No. 124, 2026

Long-term (1990-2023) reanalysis of phytotoxic ozone dose (PODY) for Sweden

Magnuz Engardt and Camilla Andersson

Reviewer: Cecilia Bennet
Department: FoU

Empty page

Summary

We present a long-term (1990-2023) reanalysis of a flux-based metrics describing ozone uptake to vegetation and the associated risk of ozone damage (Phytotoxic Ozone Dose above a flux threshold of Y, PODY). The dataset covers Sweden at 5.5 km × 5.5 km resolution and includes two generic and four specific PODY receptors (POD1gen for deciduous trees, POD1spec for birch and spruce, POD3gen for crops, and POD6spec for potato and wheat). The PODY reanalysis was constructed using the MATCH Sweden System and input meteorology from the Copernicus European Regional Reanalysis system.

PODY, for all receptors, is highest in the south of Sweden and lowest in the Scandinavian mountains. The estimated PODY for birch and spruce are well above the critical levels set by UNECE in practically all of Sweden. For wheat, the critical limits for grain yield and grain weight are exceeded in most of south and central Sweden.

We find no significant trend in PODY in most areas of Sweden, except for central Sweden for generic deciduous trees and birch (negative) and southern Sweden for potato (positive). These changes are, however, likely influenced the introduction of new observation sites in the ozone analyses. Based on the large inter-annual variation of all receptors during the 1990-2023 period we argue that there is little evidence of temporal trends in any of the receptors during the considered period.

To highlight the effects of varying ozone data as input to the PODY calculations we also performed an additional PODY reanalysis using a selection of consistent ozone observations for the period 1990-2013.

Sammanfattning

Vi presenterar en längre återanalys (1990–2023) av det flödesbaserade måttet för ozonupptag till vegetation och den tillhörande risken för ozonskador (*Phytotoxic Ozone Dose above a flux threshold of Y*, PODY). Resultaten täcker Sverige med en rumslig upplösning på 5.5 km × 5.5 km och omfattar två generiska och fyra artspecifika PODY-receptorer (POD1gen för lövträd, POD1spec för björk och gran, POD3gen för grödor samt POD6spec för potatis och vete). PODY-återanalysen togs fram med MATCH Sverigesystemet och meteorologiska indata från Copernicus European Regional Reanalysis-systemet.

PODY är högst i södra Sverige och lägst i den skandinaviska fjällkedjan för samtliga receptorer. De beräknade PODY-värdena för björk och gran ligger över de kritiska nivåer som fastställts av UNECE i praktiskt taget hela Sverige. För vete överskrids två av tre kritiska nivåer i större delen av södra och mellersta Sverige.

Vi finner ingen statistiskt signifikant trend i PODY, med undantag för mellersta Sverige för generiska lövträd och björk (negativ trend) samt södra Sverige för potatis (positiv trend). Dessa förändringar är dock sannolikt påverkade av att nya observationsstationer införts i ozonanalyserna. Mot bakgrund av den stora mellanårsvariationen för samtliga receptorer under perioden 1990–2023 bedömer vi att det finns begränsade belägg för långsiktiga trender i PODY för någon av receptorerna under den studerade perioden.

För att belysa hur variationer i ozondata som indata påverkar PODY-beräkningarna genomförde vi även en kompletterande PODY-återanalys baserad på ett urval av tidsmässigt konsistenta ozonobservationer för perioden 1990–2013.

Empty page

Table of contents

1 BACKGROUND 5

2 AIM 6

3 METHODOLOGY 6

3.1 Surface observations and calculation domain 6

3.2 PODY calculations 7

3.3 Reanalysed hourly ozone concentrations 8

3.4 Meteorology and surface data 9

3.5 Overlapping data in 2013 9

4 RESULTS 11

5 THE ROBUSTNESS OF THE PODY ANALYSES 17

6 CONCLUSIONS 28

7 APPENDIX 28

8 REFERENCES 39

9 SMHI PUBLICATIONS 41

Empty page

1 Background

The Swedish Environmental Protection Agency is responsible for environmental monitoring (*Miljöövervakning*) of air and precipitation quality in Sweden. The monitoring is conducted within the framework of the "Air Programme Area" (*Programområde Luft*) and includes several sub-programmes, including the MATCH Sweden System.

The MATCH Sweden System (e.g. Alpfjord and Andersson, 2015; Langner et al., 2019; Alpfjord Wylde et al., 2023) is an operational atmospheric chemistry transport modelling system developed at SMHI for national-scale mapping of air pollutant concentrations and deposition across Sweden. In the MATCH Sweden System, modelled air pollutant concentration fields from the Eulerian MATCH model (Multi-scale Atmospheric Transport and Chemistry; Robertson et al., 1999; Andersson et al., 2007; Bergström and Olenius, 2025) are combined with surface observations and analysed meteorology through retrospective data assimilation, to calculate analysed atmospheric concentrations and deposition of pollutants. The data assimilation of concentrations in air and precipitation is conducted to improve the spatial representation and temporal consistency of the calculated fields. The system is used for annual operational mapping of air pollutants (see https://miljoovervakning.smhi.se/), as well as long-term reanalyses (e.g. Andersson et al. 2017; 2025).

Several metrics of ground-level ozone are calculated using the MATCH Sweden System, including a flux-based metric describing ozone uptake to vegetation and the associated risk of ozone damage, known as PODY (Phytotoxic Ozone Dose above a flux threshold of Y). Compared with concentration-based metrics such as AOT40 (Accumulated Ozone exposure over a Threshold of 40 ppb), which is based on the accumulated ozone concentration above 40 ppb during daylight hours over a specified period, flux-based metrics such as PODY are generally considered more closely related to ozone-induced vegetation damage. PODY has therefore become increasingly important in international work under the UNECE Convention on Long-range Transboundary Air Pollution (CLRTAP), including assessments of critical levels for vegetation. In addition to ozone concentrations, PODY also accounts for meteorological and physical parameters controlling ozone uptake, making it a more physically realistic metric for assessing the effects of ground-level ozone on vegetation, including birch, spruce, and crops.

Flux-based ozone metrics for vegetation were first implemented in the MATCH Sweden System for generic deciduous trees and generic crops (Engardt et al., 2016). The methodology was later extended to include receptor-specific parameterizations for birch, Norway spruce, wheat and potato, including revised phenological descriptions adapted to Swedish and Scandinavian conditions (Langner et al., 2019). These developments improved the representation of vegetation-specific ozone uptake and strengthened the applicability of PODY for environmental monitoring and impact assessments in Sweden. PODY has been included in the operational environmental monitoring within the MATCH Sweden System since the monitoring year 2013 (see https://www.smhi.se/data/miljo/atmosfarskemi). The operational mapping is also reported internationally and ultimately serves as input to policy decisions regarding emission reduction measures in the European context.

In this project, a temporally consistent historical dataset of reanalysed PODY was produced and the dataset was statistically analysed with respect to trends and other characteristics.

2 Aim

The aim of the project is to utilise available ozone reanalyses and the MATCH Sweden System to produce consistent time series of PODY for six receptors relevant for Sweden, over the period 1990 through 2023. The results will cover Sweden at a spatial resolution of 5.5 km enabling detailed evaluation of the spatial variation and trends of PODY across Sweden. This data extends and compliments the currently available (2013–2024) operational assessment (*Miljöövervakning with the MATCH Sweden System*; https://miljoovervakning.smhi.se) of stomatal ozone uptake.

The extended PODY time series enable results from operational annual assessments to be put in a long-term perspective. Further, the high-resolution data set can also be used together with exposure–response relationships to estimate ozone effects on forests and crops, as well as for estimating damage and associated economic costs related to ozone exposure. Finally, the historical data provide valuable support for environmental monitoring and improve understanding of how climate variability and emission reductions can influence ozone exposure over time.

3 Methodology

To construct a time-consistent reanalysis of PODY on a high-resolution grid (5.5 km × 5.5 km) over Sweden we used reanalyzed (i.e. modelled values merged with surface observations through data assimilation techniques using the MATCH Sweden System; Andersson et al., 2015; 2017; 2025) ozone concentrations and reanalyzed meteorological data as input. PODY calculations were performed with the MATCH Sweden System using the formulations optimized for Swedish conditions (Karlsson et al., 2018), as described in Langner et al. (2019).

The results will be presented as maps showing long-term average and long-term trend retaining the original 5.5 km × 5.5 km resolution over Sweden and, for greater clarity, as tables and time series averaged over the three regions defined in Andersson et al. (2017), see Figure 1. Section 5 and section 7 also provide annual averages and timeseries for the whole of Sweden to enable extended comparison between different estimates of PODY over Sweden.

3.1 Surface observations and calculation domain

The names and locations of the observation sites used in all the ozone reanalyses and the domain for PODY-calculations are shown in the left panel of Figure 1.

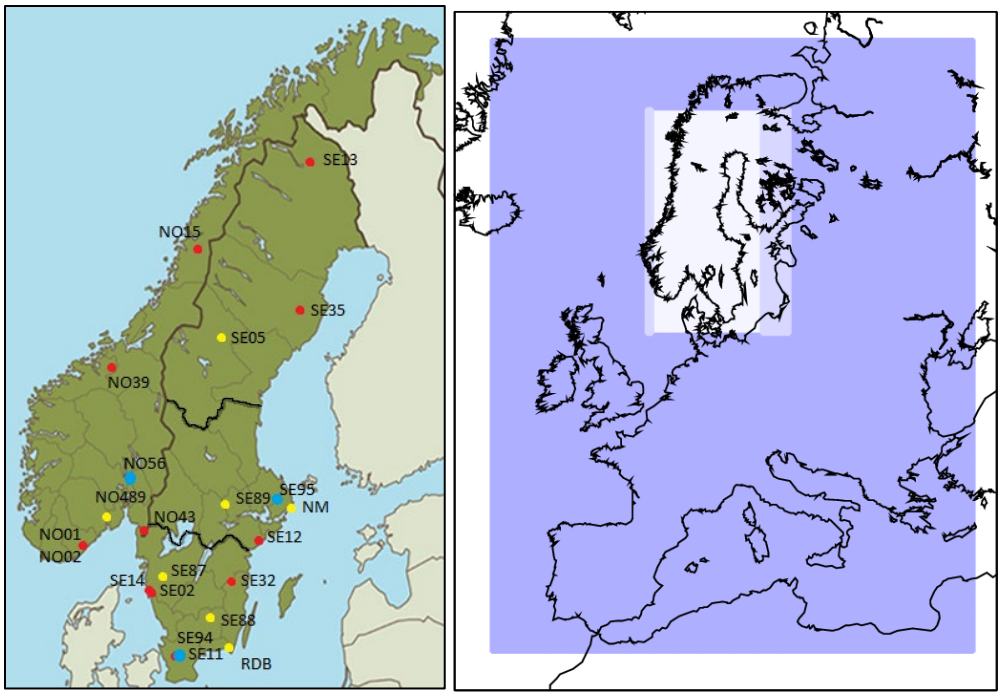

Figure 1. *The division of Sweden into three regions (North, Central and South) and sites included in the ozone reanalysis (left). Red circles are included in the strictly consistent reanalysis (1990-2013), RA_LONG. Red and yellow circles indicate all sites which are included in the RA_ALL (1990-2013). Blue circles are additional sites included in RA_MÖ. For more details on sites included for different years see Appendix, Section 7. Model domains (right): PODY reanalysis domain (fair blue domain) based on ozone reanalysis (ALL, ALLONGTERM, middle blue domain), in turn based on modelled ozone in a MATCH domain covering Europe (dark blue domain).*

3.2 PODY calculations

Receptor-specific parameterizations of stomatal ozone fluxes, F_{st}, were applied for birch, spruce, potato and wheat, including formulations for earlier ozone impacts, growing season development and stomatal response functions dependent on meteorological variables such as temperature, photosynthetically active radiation (PAR), vapour pressure deficit (VPD) and soil moisture. In addition, PODY parameterizations for generic trees and generic crops were also calculated to support broader vegetation assessments and consistency with international mapping and reporting activities.

The PODY calculations follow the flux-based methodology developed within the UNECE Convention on Long-range Transboundary Air Pollution (CLRTAP), as described in the Mapping Manual of the UNECE ICP Vegetation programme (UNECE, 2024). Here F_{st} is a function of ambient ozone concentrations close to the stomata, μ_{st}, leaf surface-, and quasi laminar resistances (r_c and r_b, respectively), as well as environmental conditions controlling the stomatal conductance, g_{st}:

$F_{st} = g_{st}\mu_{st}\frac{r_c}{r_b+r_c}$, where

$g_{st} = g_{max} \times \min\left(f_{phen}, f_{O3}\right) \times f_{light} \times max\left(f_{min}, \left[f_{temp} \times f_{VPD} \times f_{SW}\right]\right)$ and

$PODY = \sum \max\left(0, F_{st} - Y\right) \times \Delta t$.

The functions f_{xyz} all take values between 0.0 and 1.0 and are described in Langner et al. (2019) together with receptor-specific canopy heights, Y-values, g_{max} and f_{min} etc.

As described in Langner et al. (2019), f_{phen} in the MATCH Sweden system specifically make use of the phenological functions developed for Swedish conditions for birch, spruce, potato and wheat (Karlsson et al., 2018). Here, the growing season for birch and spruce is based on county-specific temperature sums together with functions incorporating latitude and day of year. f_{phen} for potato and wheat is largely based on county-based statistics of mid-anthesis of these crops.

Figure 2 describes the flow from from hourly reanalyzed ozone concentration to PODY for the respective receptors. Note that while f_{light}, f_{temp}, f_{VPD} and f_{SW} can be deduced hour by hour while the particulars of the respective receptor's growing season (f_{phen}) and premature senescence due to accumulated ozone impacts (f_{O3}) need to be precalculated for each year.

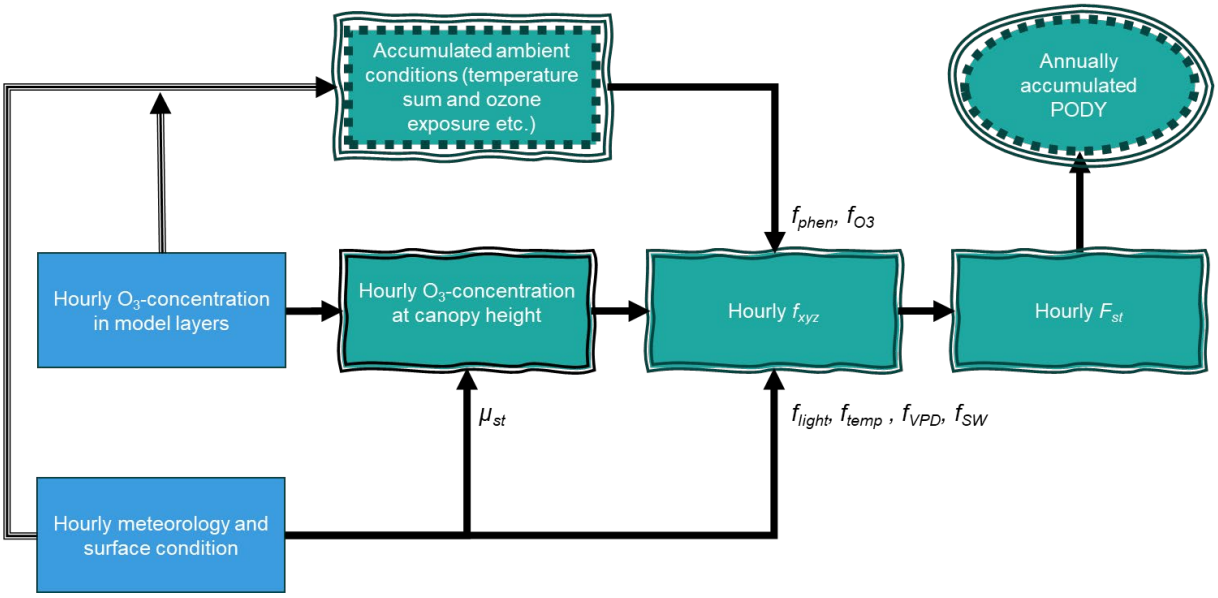

***Figure 2**. Work flow; from hourly ozone concentration to annually accumulated PODY for the various receptors. Blue areas represent input data while green areas are the results of the PODY calculations. Double frames indicate receptor-specific values while a dashed frame indicate an accumulated value over the whole year.*

3.3 Reanalysed hourly ozone concentrations

For ozone concentrations we had access to two different long-term reanalyses produced and described by Andersson et al. (2015; 2017) covering 1990 through 2013 (ALL and ALLLONGTERM). For 2013 through 2023 we had access to the publicly available data from the Swedish environmental monitoring (see https://www.smhi.se/data/luftkvalitet/datavardskap-atmosfarskemi; Alpfjord and Andersson, 2015; MÖ). All three ozone reanalyses have been produced using the MATCH Sweden System and were generated in an almost identical manner, see Table 1 below.

The input ozone reanalyses are all available on hourly resolution. The fields come on a rotated latitude-longitude grid with 0.2° × 0.2° (ca. 22 km × 22 km) grid size over the period 1990-2019 and on 0.1° × 0.1° (ca. 11 km x 11 km) grids for 2020-2023. All ozone data were interpolated to the 5.5 km × 5.5 km resolution of the current PODY calculations.

Our main results, here denoted RA_TOT and presented in Section 4, is formed from two sets of PODY reanalyses, which make use of as much ozone observations as possible, namely:

RA_TOT *(1990-2023)* = RA_ALL *(1990-2013)* + RA_MÖ *(2014-2023)*

Where RA_ALL is our PODY reanalysis covering the period 1990 through 2013 using the ALL ozone reanalysis of Andersson et al. (2017) as input and RA_MÖ (presently covering the period 2013-2024) is our PODY reanalysis extending the period through 2023 by using operational ozone reanalyses from the Swedish operational environmental monitoring (Alpfjord and Andersson, 2015) as input.

The validity of using slightly different input data in producing the input ozone concentrations for our PODY calculations is explored in Section 5 below.

3.4 Meteorology and surface data

Meteorological and surface (e.g. soil moisture) input data used in the PODY calculations were obtained from the Copernicus European Regional Reanalysis system (CERRA). The original publication (Ridal et al., 2024) provides a thorough description of the data and includes results up to 2021. The data itself is downloaded from the Copernicus Climate Data Store (CDS, https://cds.climate.copernicus.eu/datasets?q=cerra), where it is continuously augmented with recent data. As of June 2026, the data on CDS include data up through 2023, hence our PODY reanalysis ends here.

CERRA features all relevant meteorological and surface variables on a Lambert conformal conical grid with 5.5 km × 5.5 km horizontal resolution and hourly to daily time resolution. This data is internally coherent and time-consistent over the considered period. The meteorological and surface data were regridded to a 0.05° × 0.05° (5.5 km × 5.5 km) rotated latitude-longitude grid, covering Sweden that fits geometrically into the coarser (0.2° × 0.2° or 0.1° × 0.1°) ozone data (see Figure 1).

The meteorological and surface data from CERRA are used in all our calculation of the f_{xyz}-functions, which determine the stomatal conductance, g_{st} (see Langner et al., 2019) at every grid cell, at every hour. The CERRA data is also used to deduce the effectiveness of near-surface mixing, which is used to convert the reanalysed ozone concentrations to canopy layer height (20 meters above surface for the 3 tree receptors and 1 meter above surface for the 3 crop receptors).

3.5 Overlapping data in 2013

Table 1 summarizes the specifics of the various PODY reanalyses developed and used in this study. RA_LONG, RA_ALL, RA_MÖ and MÖ use reanalysed (fused modelled and observed) hourly ozone concentrations as input, while EMEP (2015) and EMEP (2025) use modelled ozone. RA_LONG and RA_ALL differ with respect to the more stringent criteria for which ozone measurements to include in the RA_LONG reanalysis but cover identical time period (see Andersson et al, 2017). RA_MÖ and MÖ cover a later period and are both based on ozone concentrations from the national operational environmental monitoring (Alpfjord and Andersson, 2015; https://www.smhi.se/data/luftkvalitet/datavardskap-atmosfarskemi), but where RA_MÖ uses the same input meteorology as RA_LONG and RA_ALL. The EMEP data are only available for generic deciduous tree and generic crops and will be used for comparison. RA_TOT is not a separate simulation but a concatenation of RA_ALL (1990-2013) and RA_MÖ (2014-2023).

Table 1. Characteristics of the different simulations. Note the overlap during 2013.

	SIMULATION PERIOD	POD MODEL	INPUT METE-OROLOGY	INPUT OZONE DATA
RA_LONG[1]	1990-2013	MATCH Sweden System Langner et al. (2019)	CERRA Ridal et al. (2024)	Fused modelled and measured hourly fields, reanalysis ALLONGTERM Andersson et al. (2017)
RA_ALL[2]	1990-2013	MATCH Sweden System Langner et al. (2019)	CERRA Ridal et al. (2024)	Fused modelled and measured hourly fields, reanalysis ALL Andersson et al. (2017)
RA_MÖ[3]	2013-2023	MATCH Sweden System Langner et al. (2019)	CERRA Ridal et al. (2024)	Fused modelled and measured hourly fields, operational reanalysis[4]
MÖ[5]	2013-2023	MATCH Sweden System Langner et al. (2019)	ECMWF-IFS, MESAN, STRÅNG	Fused modelled and measured hourly fields, operational reanalysis [6]
EMEP (2015)[7]	2013, 2014, 2015	EMEP MSC-W rv4.7 Gauss et al. (2015)	ECMWF-IFS	Modelled fields by EMEP MSC-W rv4.7 Gauss et al. (2015)
EMEP (2025)[8]	1990, 1995, 2000, 2005, 2010, 2015-2023	EMEP POD_1-IAM_DF Klein et al. (2025) Simpson et al. (2021)	ECMWF-IFS	Modelled fields by EMEP MSC-W rv5.6. Klein et al. (2025)
RA_TOT[9]	1990-2023	x	x	POD reanalyzes RA_ALL (1990-2013) RA_MÖ (2014-2023)

[1] This study.
[2] This study.
[3] This study.
[4] Swedish operational environmental monitoring mapping, produced annually. https://www.smhi.se/data/luftkvalitet/datavardskap-atmosfarskemi Alpfjord and Andersson (2015).
[5] Swedish operational environmental monitoring mapping. https://www.smhi.se/data/luftkvalitet/datavardskap-atmosfarskemi
[6] Swedish operational environmental monitoring mapping. https://www.smhi.se/data/luftkvalitet/datavardskap-atmosfarskemi
[7] Gauss et al. (2015)
[8] Klein et al. (2025)
[9] This study.

4 Results

Figure 3 and Figure 4 show maps of long term-term average PODY for trees and crops, respectively. All six receptors feature the highest values in the south of Sweden (extending up along the east coast). At high elevation sites in the Scandinavian mountains are all values low, indicating unfavourable growing conditions for the receptors considered in this study.

As already pointed out by Langner et al. (2019), practically all of Sweden exceed the "*acceptable biomass loss*" (UNECE, 2024; page 107) by a wide margin. For birch a 4 % annual reduction is expected at >5.2 mmol m^{-2} while for spruce a 2 % annual reduction is expected at >9.2 mmol m^{-2}. The exceedances are substantial and raises questions about whether the PODY-formulations for birch and spruce are correct, whether the critical levels set by the Mapping Manual are applicable to Swedish conditions, or whether the trees in Sweden actually live in an environment with such a high level of ozone-induces stress. The implementation in the MATCH Sweden System was scrutinized on several occasions and any significant impact from errors and bugs to the system has been ruled out (Andersson and Langner, 2023; Karlsson et al., 2024). These questions remain subjects to additional studies.

Sweden is generally well below the receptor-specific (UNECE, 2024) critical limits for potato (5 % reduction at > 3.8 mmol m^{-2} $POD6_{spec}$) while for wheat (5 % reduction at > 1.3-2.0 mmol m^{-2} $POD6_{spec}$) the major part of south and central Sweden exceeds 1.5 mmol m^{-2}, indicating ozone induced damages in these parts of Sweden.

Figure 5 and Figure 6 show the spatial variation of the linear trend of PODY for all receptors over the 34-year period 1990-2023[10]. There are tendencies for an increasing trend in most PODY receptors in the north of Sweden. All tree receptors feature decreases in central and southern Sweden while – in particular – POD6spec potato show increasing trends in central and southern Sweden. Although a large area in central Sweden features significant negative trends of all tree receptors, the spatially averaged trends are generally not statistically significant, see Table 2.

As evident from Figure 7 and Figure 8 is the interannual variation large for all receptors in all regions, which obscures potential long-term trends. From Figure 7 and Figure 8 it can be noted that the year-to-year variations in PODY for the crop receptors are particularly large, in relative terms – a consequence of their higher thresholds (*Y*-values). This large inter-annual variation masks the comparatively large (and thus mostly insignificant) trend in POD6spec potato, which increase 40 to 54 % in our three Swedish regions over the considered 34-year period.

A final thing to bear in mind is that both the long-term averages and the long-term trends of PODY have been calculate over all 5.5 km × 5.5 km land cells of Sweden. The maps and regional trends in Table 2 will therefore likely not represent the conditions where, say, spruce grow naturally or where farmers actually grow potato. Refinement to even higher resolution was deemed to be outside the scope of the present project.

[10] Seemingly strong trends in some coastal areas are, yet to be resolved, technical problems arising when merging trend data over water with land data and should be ignored.

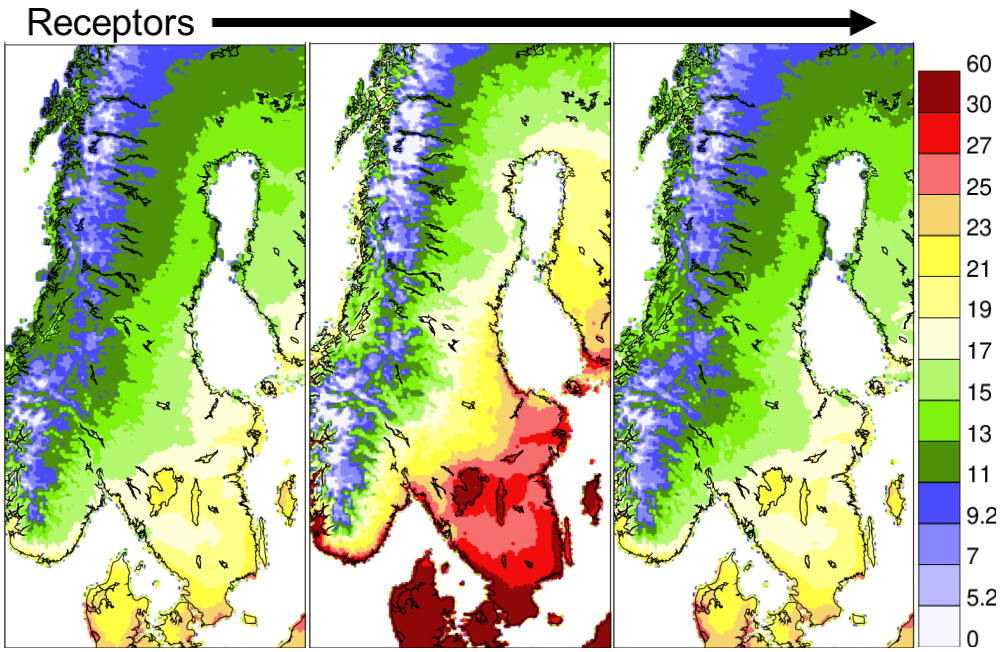

Figure 3. *Long-term average (1990-2023) annually accumulated PODY for (left) POD1gen deciduous trees, (middle) POD1spec birch and (right) POD1spec spruce. Data are based on the reanalysis including all observations (RA_TOT). Unit: mmol m^{-2}.*
Note different color scales in Figure 3 and Figure 4.

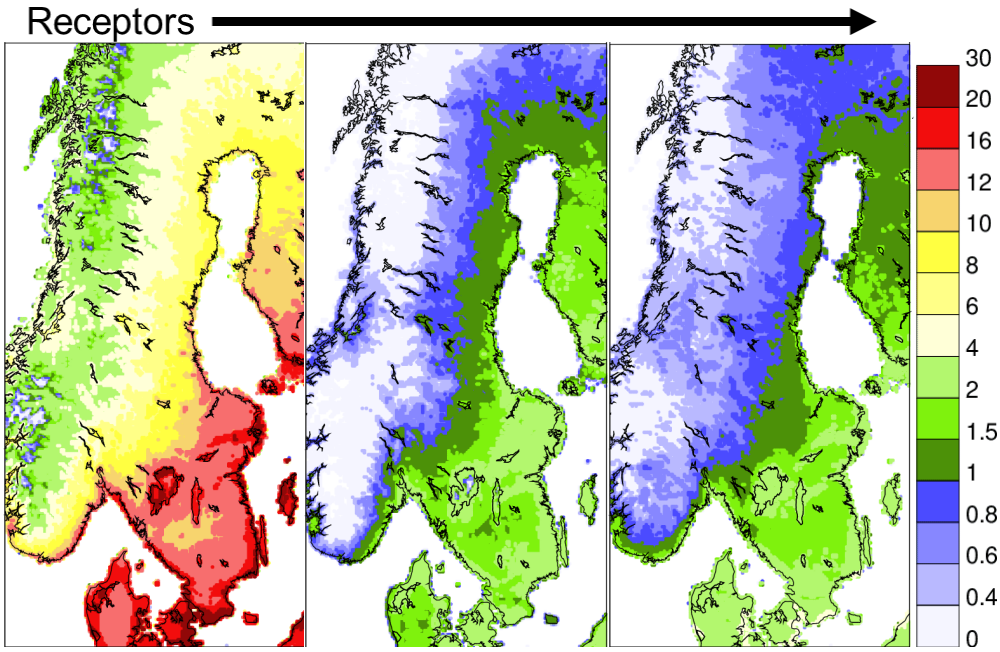

Figure 4. *Long-term average (1990-2023) annually accumulated PODY for (left) POD3gen crops, (middle) POD6spec potato and (right) POD6 spec wheat. Data are based on the reanalysis including all observations (RA_TOT). Unit: mmol m^{-2}.*
Note different color scales in Figure 3 and Figure 4.

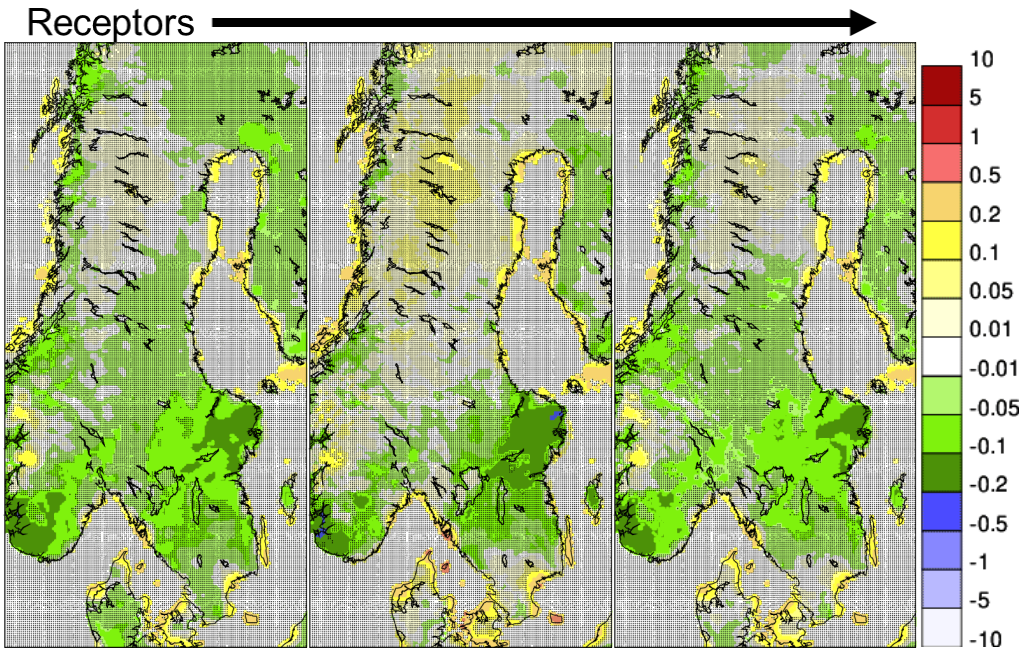

Figure 5. *Long-term (1990-2023) linear trend in PODY for: (left) POD1gen deciduous trees, (middle) POD1spec birch and (right) POD1spec spruce. Data are based on the reanalysis including all observations (RA_TOT). Unit: mmol m^{-2} year^{-1}.*

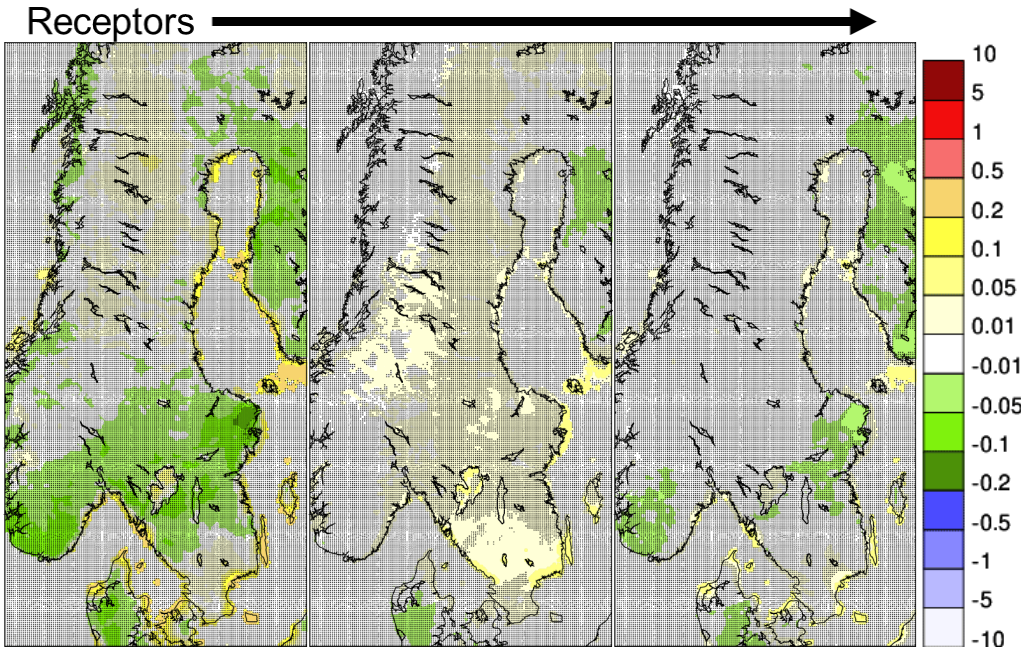

Figure 6. *Long-term (1990-2023) linear trend in PODY for: (left) POD3gen crops, (middle) POD6spec potato and (right) POD6 spec wheat. Data are based on the reanalysis including all observations (RA_TOT). Unit: mmol m^{-2} year^{-1}.*

Table 2. *Long-term linear trend in six PODY receptors for (1990-2023) in mmol m^{-2} $year^{-1}$. Bold numbers marked with an asterisk are significant to $p<0.05$. Values within parenthesis are percentual change[11] over the 34-year period. Data are based on the reanalysis including all observations (RA_TOT) considering all cells with at least 20 % land.*

RECEPTOR	NORTH	CENTRAL	SOUTH
POD1GEN DECIDUOUS TREE	0.00 (0 %)	**-0.06*** (-12 %)	-0.03 (-5 %)
POD1SPEC BIRCH	+0.03 (+9 %)	-0.05 (-7 %)	-0.01 (-1 %)
POD1SPEC SPRUCE	0.00 (+1 %)	**-0.06*** (-12 %)	-0.01 (-3 %)
POD3GEN CROPS	+0.01 (+9 %)	-0.03 (-8 %)	+0.01 (+3 %)
POD6SPEC POTATO	+0.01 (+54 %)	+0.02 (+40 %)	**+0.03*** (+54 %)
POD6SPEC WHEAT	0.00 (+11 %)	0.00 (-6 %)	+0.01 (+9 %)

[11] Calculated as the respective regional trend (in mmol m^{-2} $year^{-1}$) divided by the long-term average (in mmol m^{-2}) of the corresponding region and multiplied with 33×100 to get percentual change over the full period.

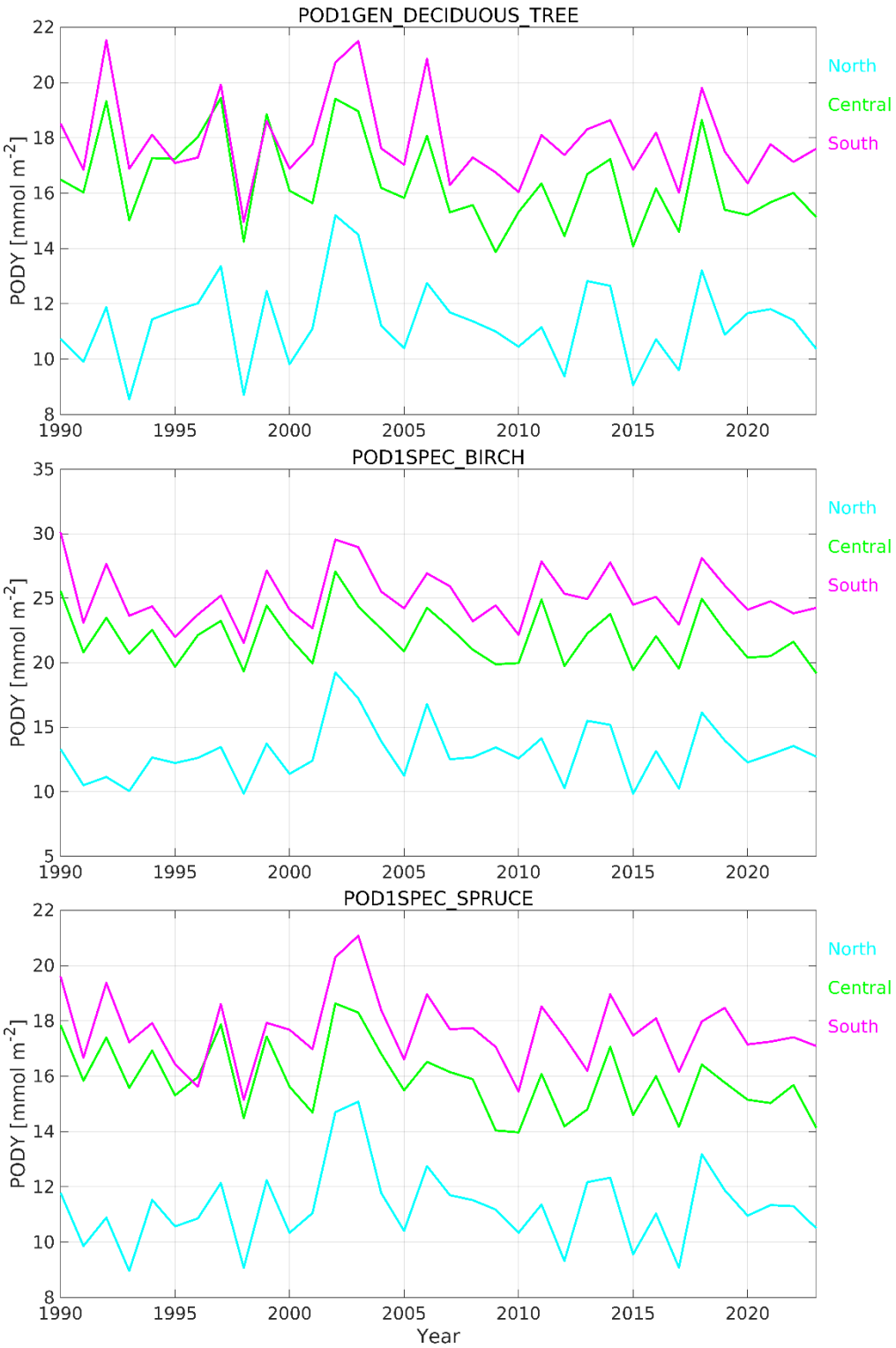

Figure 7. *Annual variation (1990-2023) of: (top) POD1gen deciduous trees; (middle) POD1spec birch; (bottom) POD1spec spruce. Data are based on the reanalysis including maximum number of observations (RA_TOT). The three curves represent the different regions of Sweden marked in Figure 1.*
Unit: mmol m^{-2}.

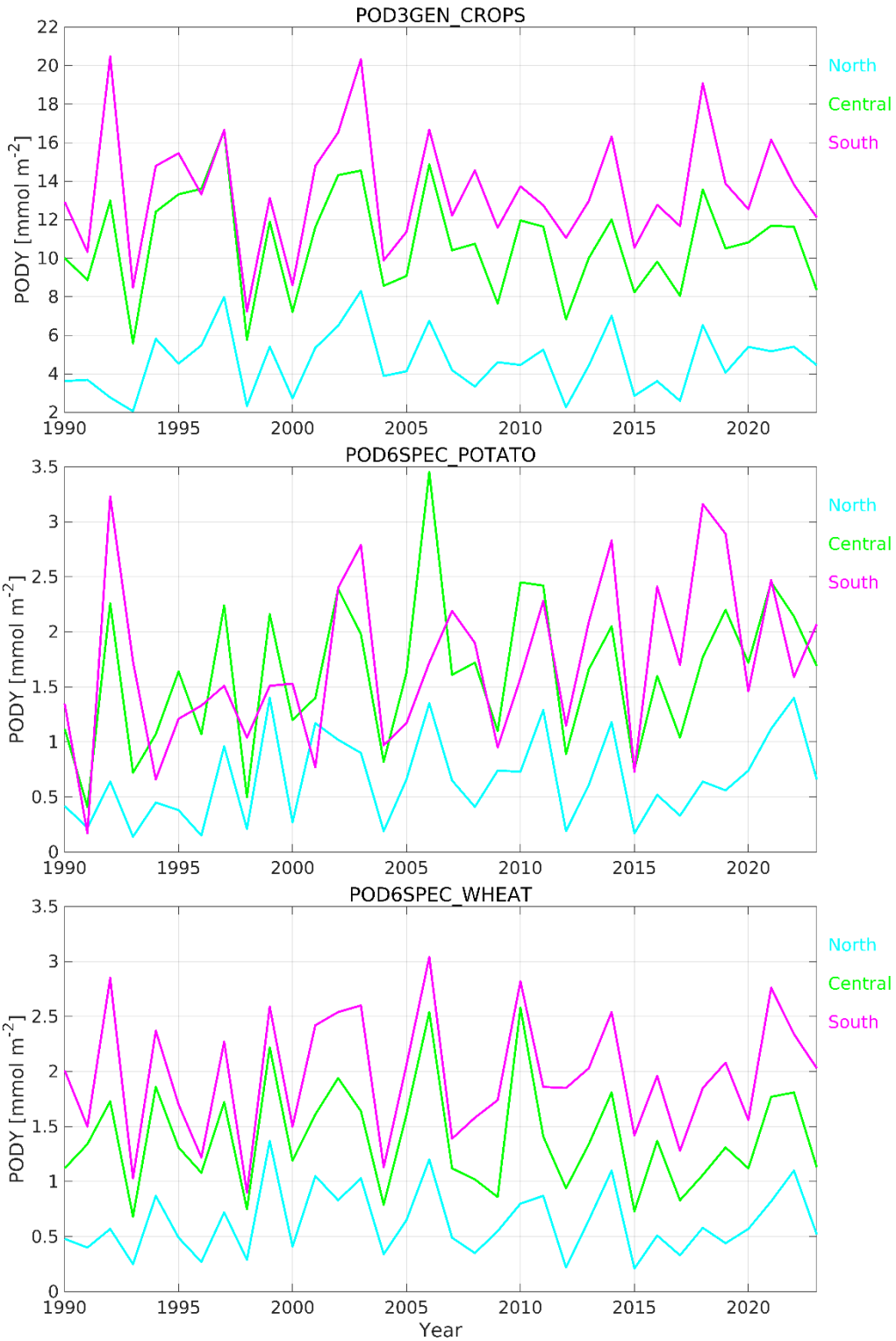

Figure 8. *As Figure 7 but: (top) POD3gen crops, POD6spec potato, POD6spec wheat.*

5 The robustness of the PODY analyses

In this section we discuss the implications of using slightly different ozone data in our PODY reanalyses and compare our results with earlier studies.

Figure 9 summarizes the differences by showing PODY averaged over the whole of Sweden for the year 2013, where we have overlapping ozone data for a number of different PODY calculations. The results of the different calculations are generally comparable for the different receptors and there are no pervasive features, although discrepancies are to be expected following the differences in the driving ozone concentrations, meteorology and surface data. We can, for example, recall that MÖ uses different meteorological input data compared to our three reanalyses and its soil moisture data is valid at 1-3 meters depth while in our PODY reanalyses we have used soil moisture at 0.8-1.0 meters depth. A shallower depth is expected to result in reduced F_{st} due to a more variable and typically drier soil. However, the differences between, say, RA_LONG and MÖ appears coincidental: For deciduous trees, birch and wheat are MÖ slightly lower, while MÖ is clearly higher than RA_LONG for crops and potato but very similar for spruce. Likewise, the EMEP (2015) data are much higher for deciduous trees but clearly lower for crops.

Figure 10 and Figure 11 show the spatial distribution of PODY for our six receptors for the year 2013. A visual inspection of the maps shows there is hardly any differences in any part of Sweden, except for parts of the mountainous areas where the coarser resolution of MÖ produces a slightly different picture. There are also tendencies for PODY being slightly higher (in confined coastal areas close to Öland, Gotland and the Åland archipelago) for some of the receptors in RA_MÖ than in RA_ALL and RA_LONG.

Figure 12 and Figure 13 show long-term average PODY for the receptors considered in this study. The figures demonstrate the similarity between, in particular, the RA_LONG and the RA_ALL, both covering the period 1990-2013. The rightmost panels in both figures depicts RA_TOT, which have already been shown in this report (Figure 3 and Figure 4). RA_TOT covers an extended period (1990-2023) and should not be expected to be identical to the other two PODY reanalyses. Still, it is very difficult to identify any areas where the long-term averages differ substantially between the three re-analyses, indicating that the long-term averages presented in Figure 3 and Figure 4 are robust and that temporal trends are minor due to the fact that the addition of 10 years of data hardly alter the results.

Figure 14 and Figure 15 present a seemingly different picture. The figures show long-term trends in PODY for the receptors considered in this study. While the overall impression is that there is barely any significant trend over the periods, there are clear differences looking into the details, particularly when comparing significant trends between the three datasets. There are substantial differences in the linear trend of PODY in some parts of Sweden between the RA_LONG and RA_ALL (the two leftmost columns), which both cover the same period and where RA_LONG is time-consistent in terms of observation sites (see Andersson et al., 2017). These differences are particularly pronounced in the central part of Sweden related to the introduction or termination of ozone sites used in the ozone reanalysis. As also evident from Table 3, are the regionally averaged linear trends in central Sweden noticeably different between RA_LONG and RA_ALL. For POD1spec BIRCH we even see an increasing trend in RA_LONG and a decreasing trend in RA_ALL, albeit none of these trends are statistically significant. Appendix, Figure A1, shows data capture by year for individual observation sites included in RA_LONG, RA_ALL and RA_MÖ respectively. Particularly central Sweden appears to be impacted by the closure of Aspvreten, and introduction of Norunda, Norr Malma and Grimsö. Similarly, POD6spec for potato in southern Sweden (and the Scandes) is likely also due to changes in observation sites in the time period. It is out of the scope of this study to in detail study the impact of these changes.

The rightmost panels in Figure 14 and Figure 15 depict RA_TOT which have already been shown in this report (Figure 5 and Figure 6) . RA_TOT covers an extended period (1990-2023) and should not be expected to be identical to the other two PODY reanalyses. Table 3 reveals that while RA_LONG and RA_ALL is similar in northern Sweden RA_TOT consequently shows a different (smaller) trends.

None of the calculated trends in northern Sweden are, however, significant. For southern and central Sweden, RA_TOT often feature a stronger negative trend than RA_LONG and there are a handful of instances with significant negative (or positive trends). In all these instances are the signs of the trends in all three reanalyses identical. Considering details in RA_TOT compared to RA_ALL, there is also a positive trend along the greater Baltic Sea coastline, in similar locations as differences were identified for 2013. These trends are also likely artificial and due to changes in reanalysed ozone between RA_ALL and RA_MÖ.

The significant trends in RA_TOT for POD1 in central Sweden, and POD6spec potato in southern Sweden are thus likely artificial, due to the large number of changing sites in the 1990-2023 period. A user in need of a strictly time-consistent dataset should consider the RA_LONG dataset, available for 1990-2013. It would have been possible to construct a long-term time-consistent dataset for 1990-2023, including only sites that have been available throughout the whole time period. Such a dataset would however only include 2 Swedish sites if restricted to the same location, or 4 sites if Råö and Rörvik, and Vavihill and Hallahus can be considered as interchangeable. For this study the benefit of the additional effort was deemed as not worthwhile, considering the few Swedish sites fulfilling the criteria. This illustrates the problem with changing location of observational sites over time and the importance of maintaining long-term sites for trend analysis purposes.

Figure 16 and Figure 17, finally, show regionally averaged annual variation of PODY for the receptors considered in this study. The figures are shown to illustrate the growing difference between the RA_LONG and the RA_ALL simulations, but also how small this difference is compared to the interannual variation of PODY stemming from variations in meteorology and surface data.

The different reanalyses show very similar inter-annual variation while the difference between the various reanalyses remain relatively small (and practically absent in the north of Sweden). The difference in PODY for a particular year and receptor is always much less than, say, 10 % while year-to-year variations due to differences in meteorology is on the order 30-40 % for the tree receptors and often over 100 % for the crop receptors.

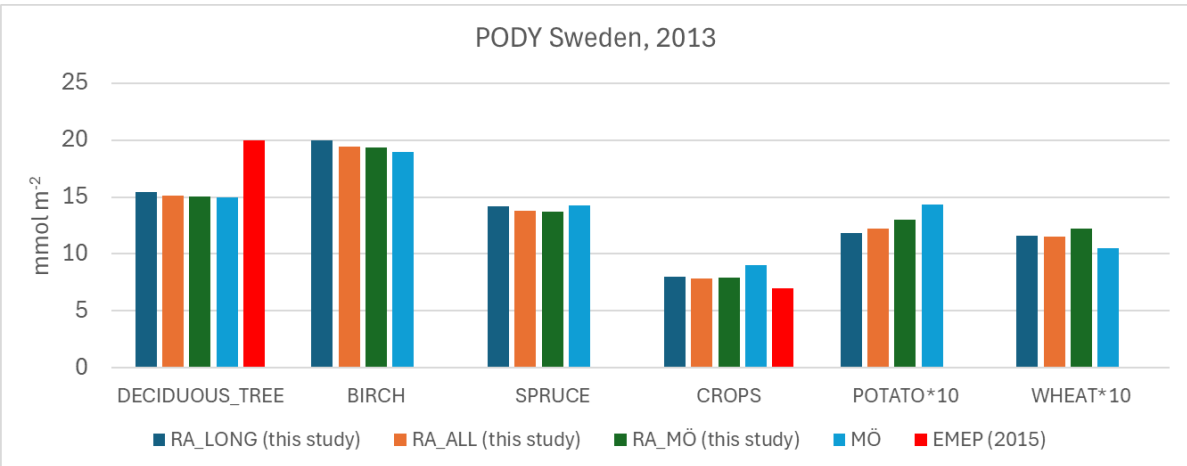

Figure 9. *PODY for six receptors averaged over the whole Swedish land area for the year 2013 using different input data, see Table 1. Note that PODY6spec POTATO and PODY6spec WHEAT has been multiplied by 10 to increase legibility.*

Table 3. *Linear trend (mmol m^{-2} $year^{-1}$) in six PODY metrics for three different reanalyses RA_LONG and RA_ALL (1990-2013) and RA_TOT (the total dataset; 1990-2023). RA_TOT is RA_ALL (1990-2013) padded with RA_MÖ (2014-2023). Bold numbers marked with an asterisk are significant to $p<0.05$. Red and blue entries highlight positive and negative changes, respectively.*

	North			Central			South		
	1990-2013		1990-2023	1990-2013		1990-2023	1990-2013		1990-2023
Receptor	RA_ LONG	RA_ALL	RA_TOT	RA_ LONG	RA_ALL	RA_TOT	RA_ LONG	RA_ALL	RA_TOT
POD1GEN DECIDUOUS TREE	0.03	0.03	0.00	-0.03	-0.08	**-0.06***	-0.02	-0.03	-0.03
POD1SPEC BIRCH	0.11	0.10	0.03	0.04	-0.03	-0.05	0.01	0.00	-0.01
POD1SPEC SPRUCE	0.04	0.03	0.00	-0.03	**-0.08***	**-0.06***	-0.01	-0.02	-0.01
POD3GEN CROPS	0.02	0.02	0.01	-0.01	-0.04	-0.03	-0.02	-0.03	0.01
POD6SPEC POTATO	0.02	0.02	0.01	0.03	0.03	0.02	0.02	0.02	**0.03***
POD6SPEC WHEAT	0.01	0.01	0.00	0.01	0.01	0.00	0.01	0.01	0.01

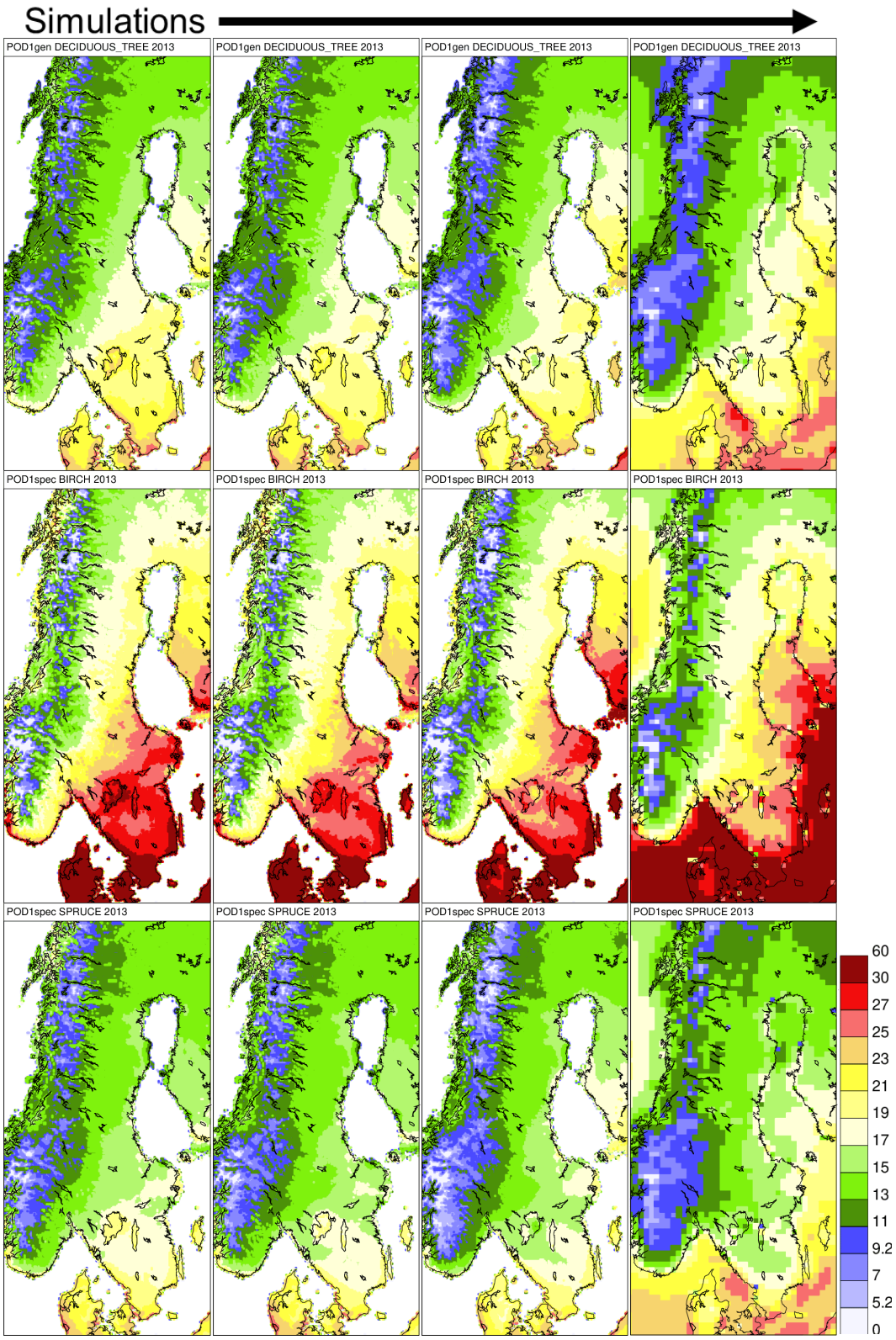

Figure 10. *PODY for different tree receptors for the year 2013 using different input data. Left column: RA_LONG, middle left: RA_ALL, middle right: RA_MÖ and right: MÖ. Top row: POD1gen deciduous trees. Middle row: POD1spec birch. Bottom row: POD6spec wheat. Note different color scales in Figure 10 and Figure 11.*

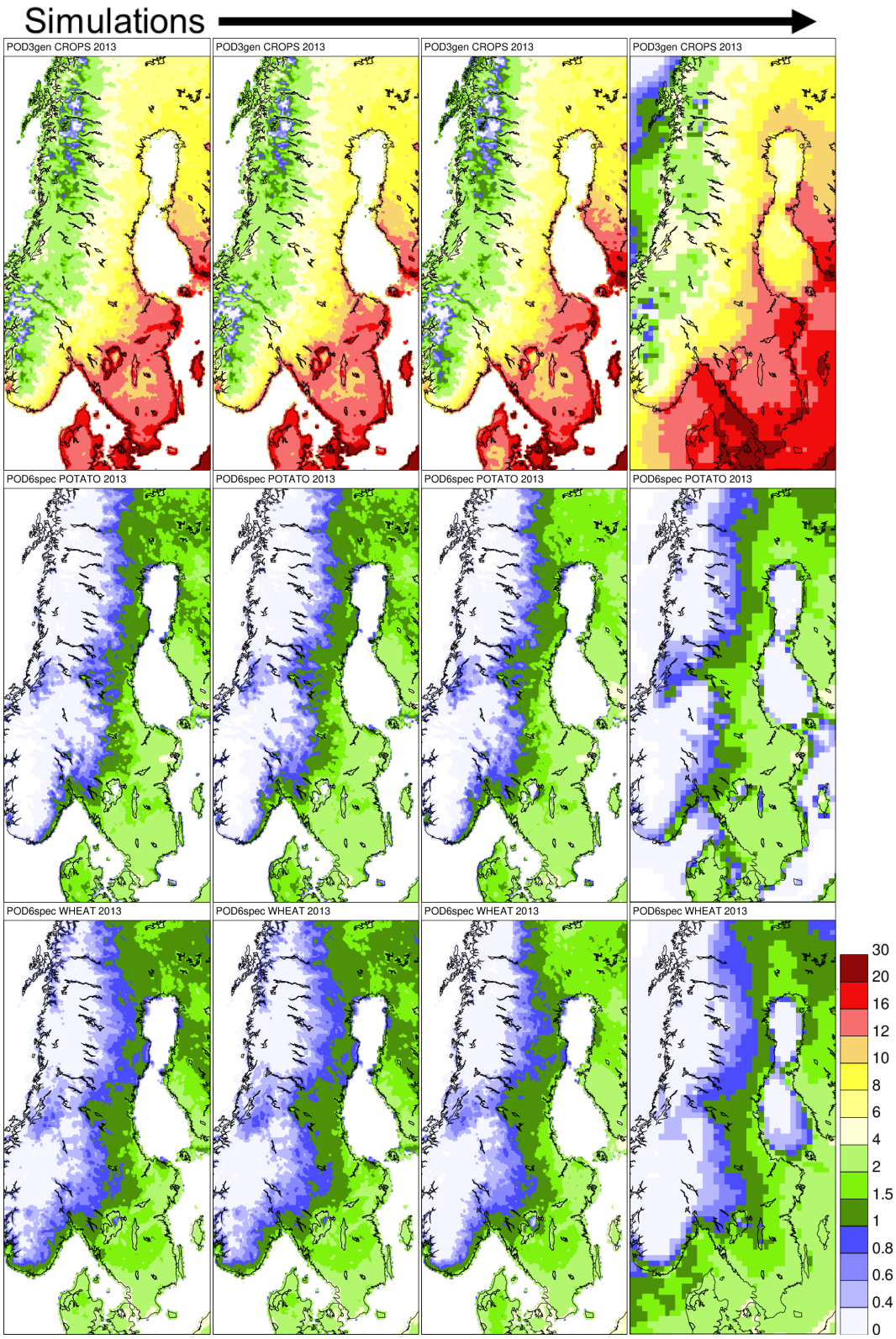

Figure 11. *PODY for crop receptors for the year 2013 using different input data. Left column: RA_LONG, middle left: RA_ALL, middle right: RA_MÖ and right: MÖ. Top row: POD3gen crops. Middle row: POD6spec potato. Bottom row: POD6spec wheat. Note different color scales in Figure 10 and Figure 11.*

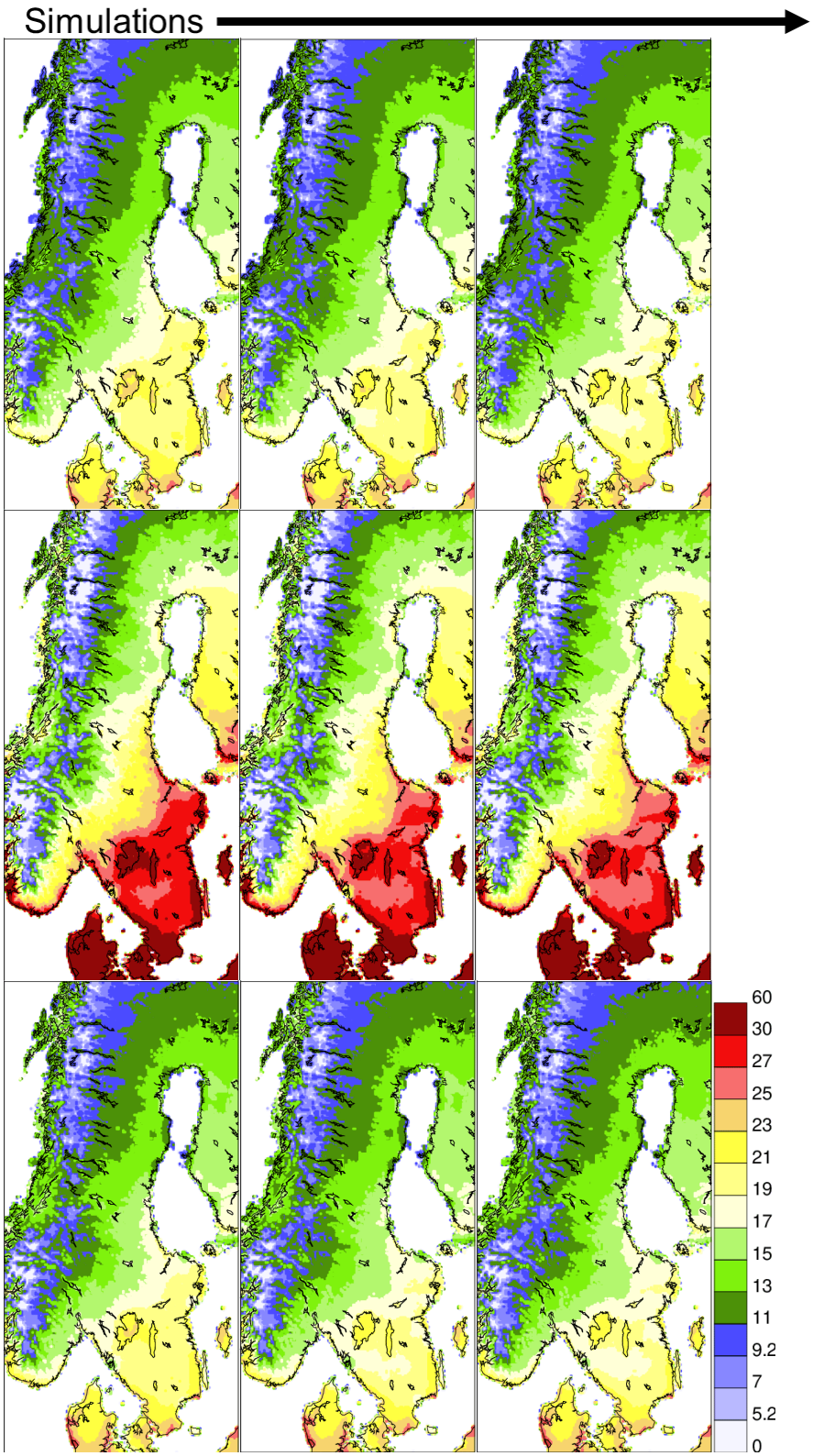

Figure 12. *Period mean annual POD1gen deciduous trees (top), POD1spec birch (middle) and POD1spec spruce (bottom). Left column period means based on RA_LONG (1990-2013), middle column based on RA_ALL (1990-2013) and right column based on RA_TOT (1990-2023). Unit: mmol m^{-2}. Note different color scales in Figure 12 and Figure 13.*

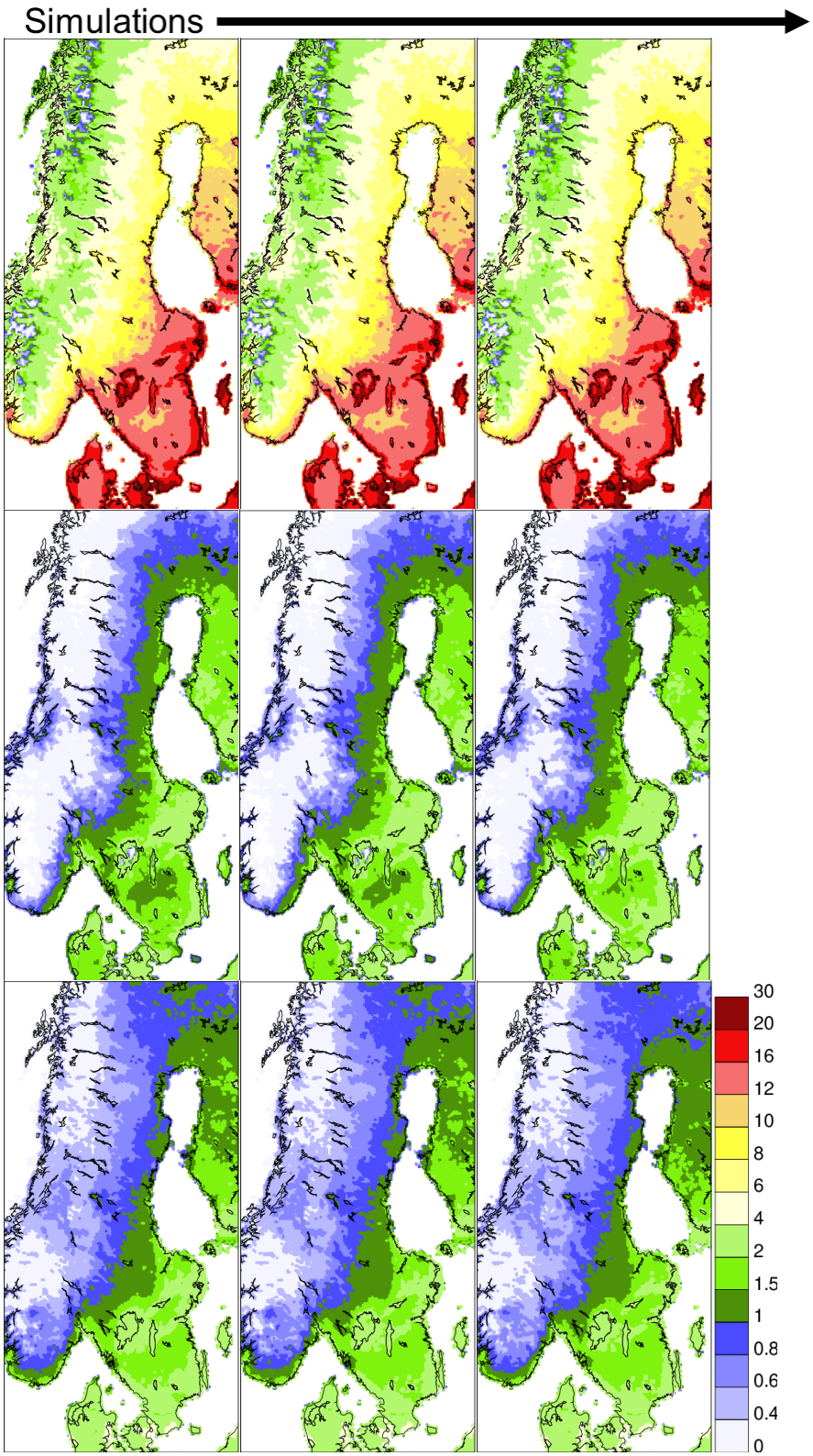

Figure 13. *Period mean annual POD3gen crops (top), POD6spec potato (middle) and POD6spec wheat (bottom). Left column period means based on RA_LONG (1990-2013), middle column based on RA_ALL (1990-2013) and right column based on RA_TOT (1990-2023) Unit: mmol m^{-2}. Note different color scales in Figure 12 and Figure 13.*

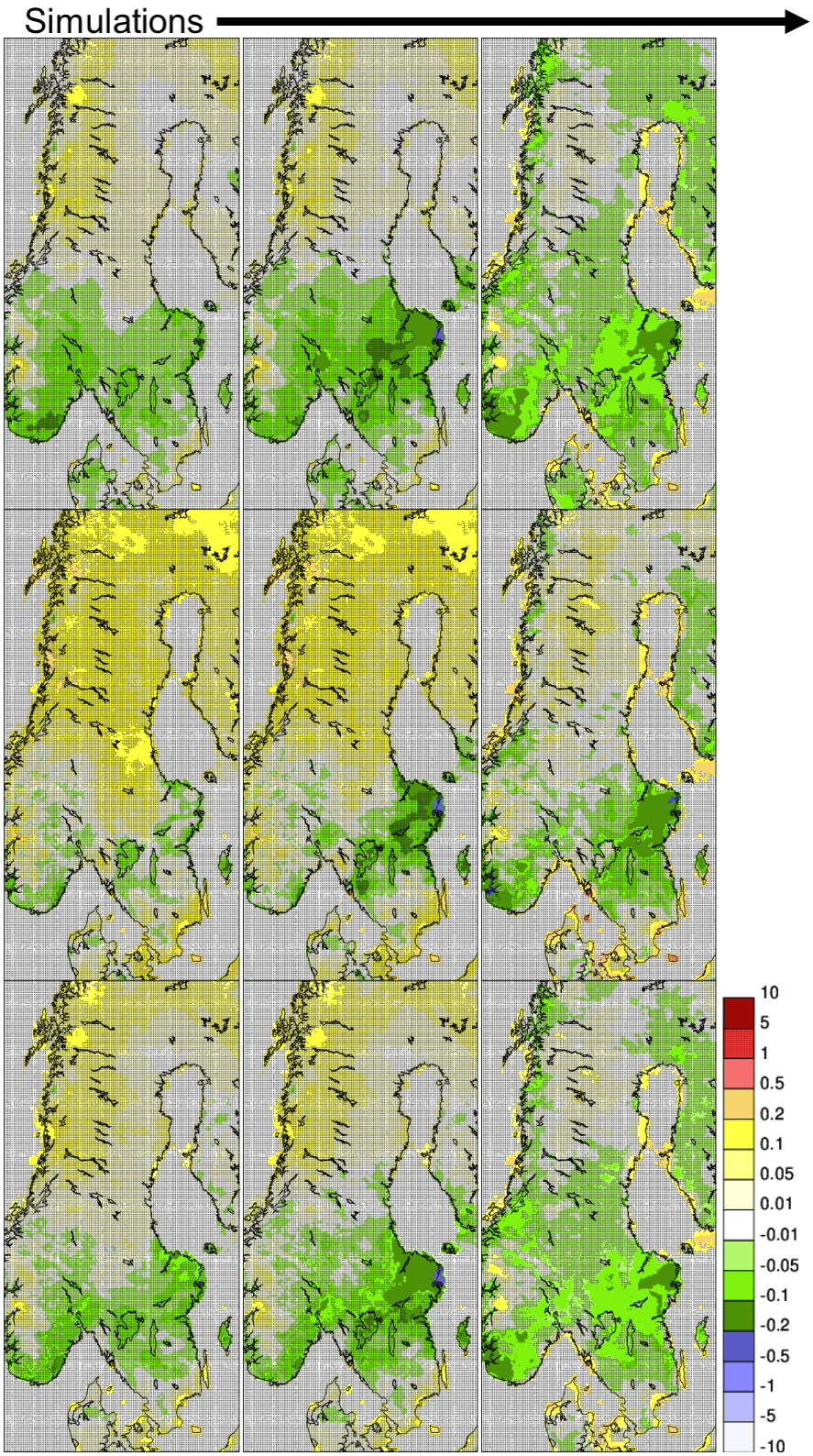

Figure 14. *Linear trend (mmol m^{-2} year^{-1}) in POD1 metrics for different tree receptors for the three different reanalyses constructed in this study. Left column: RA_LONG (1990-2013). Middle column: RA_ALL (1990-2013). Right column: RA_TOT (1990-2023). Top to bottom rows: POD1gen deciduous trees, POD1spec birch, POD1spec spruce. Insignificant trends (p>0.05) are stippled.*

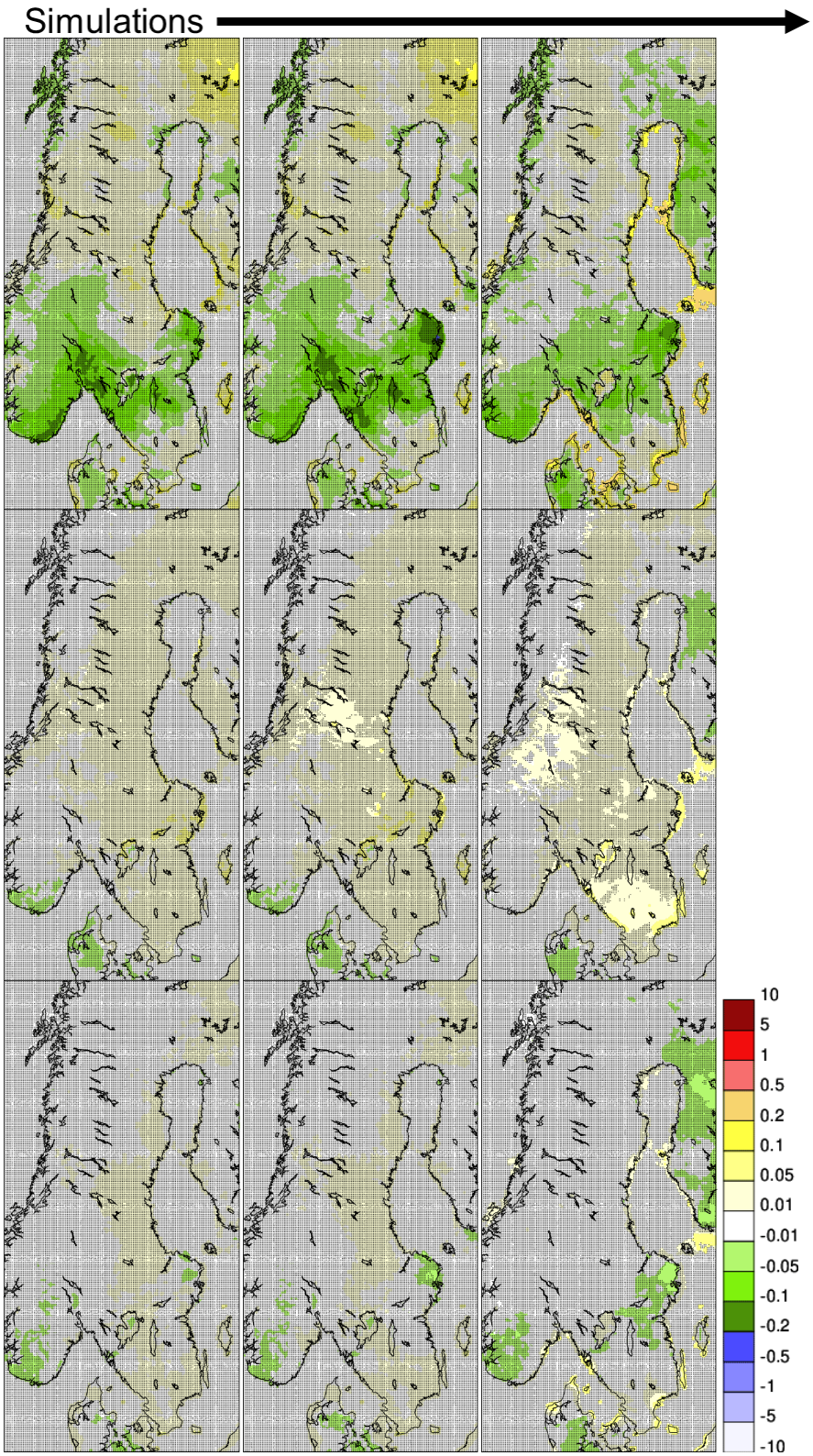

Figure 15. *Linear trend (mmol m^{-2} year^{-1}) in PODX metrics for different crop receptors for the three different reanalyses constructed in this study. Left column: RA_LONG (1990-2013). Middle column: RA_ALL (1990-2013). Right column: RA_TOT (1990-2023). Top to bottom rows: POD3gen crops, POD6spec potato, POD1spec wheat. Insignificant trends (p>0.05) are stippled.*

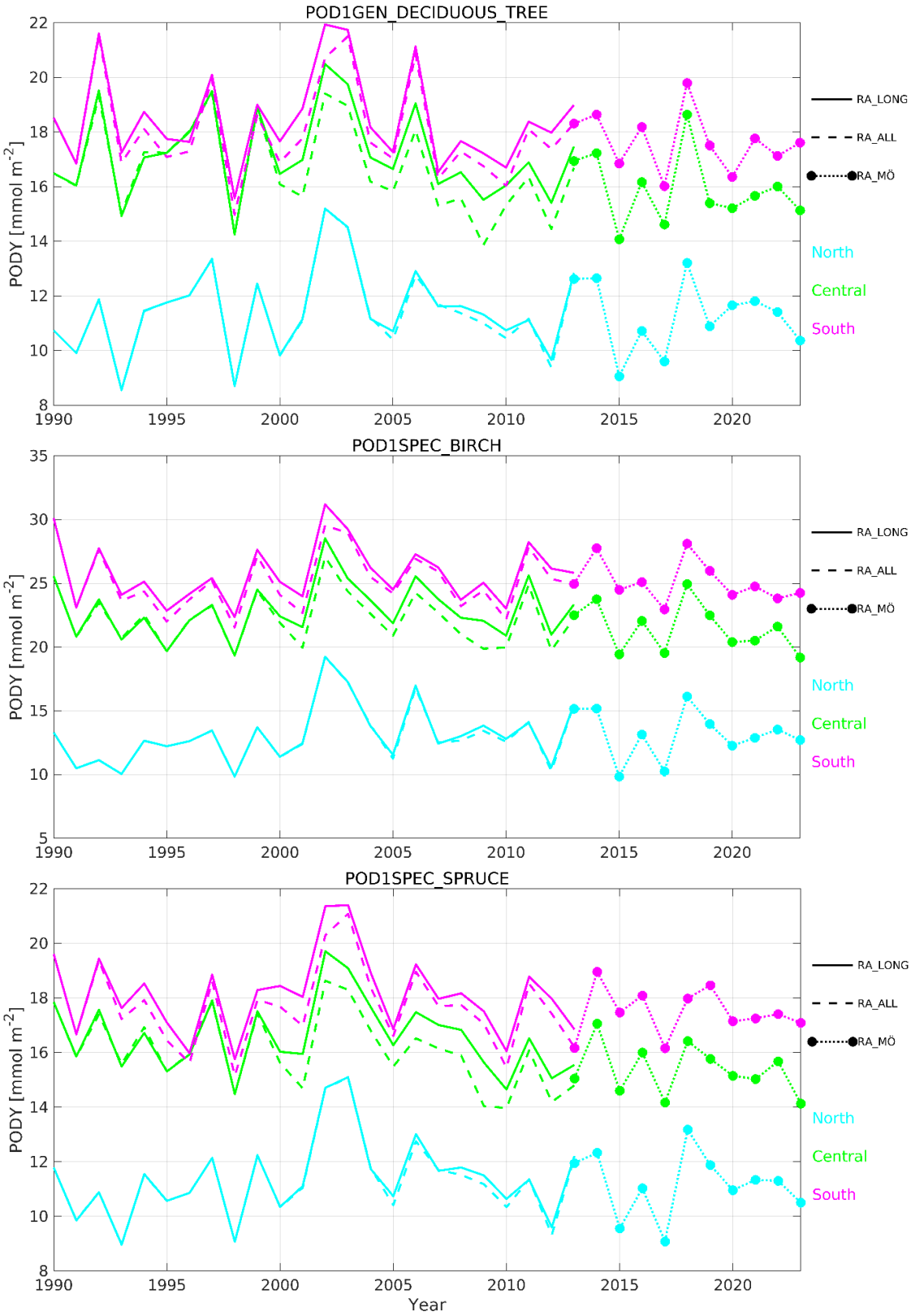

Figure 16. *Annual variation (1990-2023) of: (top) POD1gen deciduous trees; (middle) POD1spec birch; (bottom) POD1spec spruce. The different lines represent the different reanalysis data sets described in Table* 1. *The three colors represent the different regions of Sweden marked in Figure 1. Unit: mmol* m^{-2}.

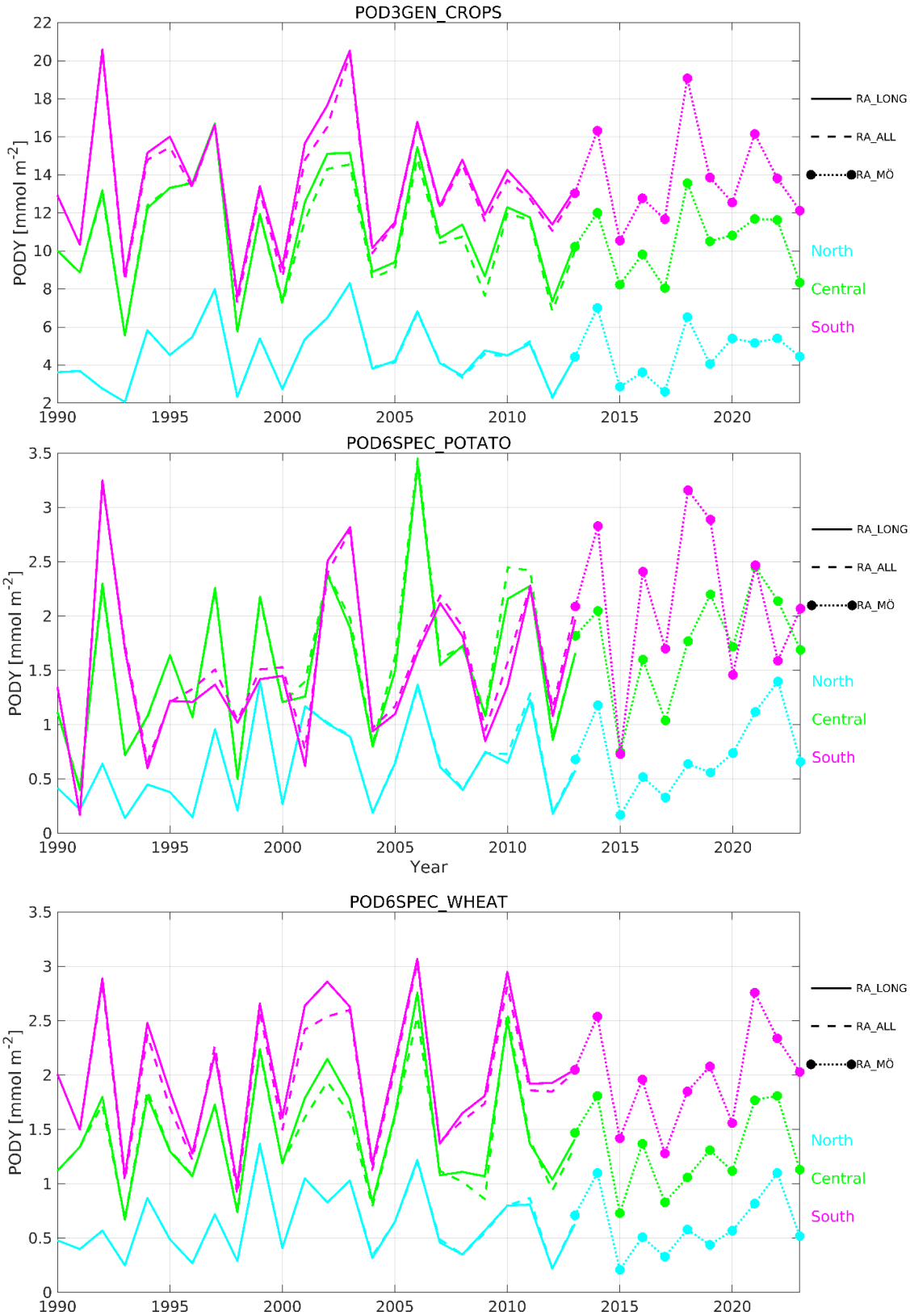

Figure 17. *As Figure 16 but: (top) POD3gen crops; (middle) POD6spec potato; (bottom) POD6spec wheat.*

6 Conclusions

In this report we present a long-term (1990-2023) reanalysis of Phytotoxic Ozone Dose above a flux threshold of Y (PODY). The dataset covers Sweden at 5.5 km × 5.5 km resolution and includes two generic and four specific PODY receptors (POD1gen for deciduous trees, POD1spec for birch and spruce, POD3gen for crops, and POD6spec for potato and wheat). The PODY reanalysis was constructed by the MATCH Sweden System using input meteorology from the Copernicus European Regional Reanalysis system and ozone data from modelled ozone concentrations merged with observations (ozone reanalyses).

The results are available as gridded fields for each consecutive year and presented in this report as maps showing the spatial variation in mean values and trends or averaged over the whole of Sweden or three different regions of Sweden (North, Central and South).

PODY, for all receptors, is highest in the south of Sweden and lowest in the Scandinavian mountains. The estimated PODY for birch and spruce are well above the critical levels set by UNECE in practically all of Sweden. For wheat, the critical limits for grain yield and grain weight are exceeded in most of south and central Sweden.

Based on the large inter-annual variation of all receptors during the studied period, we argue that there is little evidence of temporal trends in PODY for any of the receptors during the considered period. A statistical analysis of the long-term (1990-2023) data could only detect significant trends ($p<0.05$) for POD1gen deciduous trees and POD1spec spruce in central Sweden (-0.06 mmol m^{-2} $year^{-1}$ for both receptors) and for POD6spec potato in southern Sweden (+0.03 mmol m^{-2} $year^{-1}$). In a separate PODY calculation for 1990-2013, where we used ozone data from a strictly consistent ozone reanalysis (using a smaller but unchanging subset of stations), we show that some of the trends in south and central Sweden are likely influenced by the introduction of new observation sites in the ozone reanalyses used in our long-term reanalysis.

The presented PODY data are the results of modelling efforts and cannot be evaluated by direct comparison with observations. We have, however, compared our results with independent calculations performed by the EMEP system (Gauss et al., 2015; Klein et al., 2025). This is not an evaluation, but indicates robustness of the respective estimates. We note that our POD1gen deciduous tree is consequently ca. 20 % lower than EMEP's calculations while our POD3gen crops is ca 20 % higher than EMEP's calculations. Time series (shown in the Appendix) of POD1gen deciduous tree and POD3gen crops show very similar year-to-year variations in our reanalysis and the published EMEP results. Our reanalysis has likewise a similar year-to-year variability as the operationally produced PODY data available at SMHI's website while the absolute values may differ to a similar extent.

We conclude that ozone concentrations are the determining factor for PODY levels, while the meteorological variability controls the interannual variations.

7 Appendix

In this appendix we include additional supporting figures and tables:

- **Figure A1.** Ozone observation sites used in RA_TOT, including their annual capture.
- **Figures A2-A4**. Comparison of different datasets for PODY for 1990-2023 averaged over three regions.
- **Figures A5-A10**. Percentiles of PODY based on RA_TOT.
- **Figures A11.** Annually accumulated POD1gen deciduous trees.

		1990	1991	1992	1993	1994	1995	1996	1997	1998	1999	2000	2001	2002	2003	2004	2005	2006	2007	2008	2009	2010	2011	2012	2013	2014	2015	2016	2017	2018	2019	2020	2021	2022	2023
		0	0	0	0	0	0	0	0	0	0	0	0	0	0	0	0	99	99	99	99	98	90	99	99	99	97	0	0	99	99	99	99	98	99
		82	88	87	92	89	94	96	97	97	91	84	87	95	96	95	96	94	91	95	99	95	93	98	93	98	94	0	0	0	0	0	0	0	0
		97	99	95	98	98	98	99	99	98	97	99	97	0	0	0	0	0	0	0	0	0	0	0	0	99	98	0	0	0	0	0	0	0	0
		0	0	0	0	0	0	0	0	0	0	0	0	98	98	99	98	99	99	99	99	99	98	99	98	0	0	99	99	99	97	99	99	97	99
		0	0	0	0	0	0	0	0	0	0	0	0	0	0	58	98	99	97	96	99	99	99	99	98	93	99	99	99	99	95	99	99	98	96
		98	94	99	98	99	97	96	98	98	98	98	99	98	98	99	96	98	96	97	97	98	98	97	93	99	99	0	0	0	0	0	0	0	0
		0	0	0	0	0	0	0	0	0	0	0	0	0	0	0	0	0	0	0	0	0	0	0	0	0	0	98	99	99	99	98	98	99	99
		30	95	96	93	97	96	99	99	99	99	99	99	99	99	99	99	99	98	97	99	99	99	92	98	99	99	99	99	99	99	99	94	96	99
		98	96	95	97	98	96	98	98	99	95	99	95	98	99	99	94	95	95	98	99	98	99	91	95	0	0	0	0	0	0	0	0	0	0
		95	97	95	99	98	99	99	99	99	99	97	99	99	98	99	99	97	98	98	97	98	96	96	99	99	99	99	99	99	99	94	99	99	98
		0	0	0	0	0	0	0	0	0	0	41	96	99	99	98	99	99	99	99	99	99	99	99	99	97	99	97	99	98	99	96	99	99	98
		0	0	0	97	99	49	89	99	99	74	99	94	0	0	44	0	0	97	99	99	87	0	58	95	86	98	98	97	98	98	95	98	96	99
		0	0	0	0	0	0	0	0	0	0	0	47	34	20	44	49	49	50	49	49	50	48	49	99	99	99	99	99	98	98	99	99	98	98
		0	0	0	0	0	0	0	0	0	0	0	0	0	0	0	0	0	0	0	0	0	0	0	0	0	0	0	0	78	98	99	96	78	97
		0	0	0	0	0	0	0	0	0	0	0	0	0	0	0	0	0	0	0	0	0	0	0	55	0	0	97	84	99	98	99	99	99	97
		98	99	88	80	94	90	96	97	99	99	99	99	98	98	98	98	98	99	98	95	0	0	0	79	85	99	99	95	97	99	98	99	97	98
		0	0	0	0	0	0	0	0	0	0	0	0	0	0	0	0	0	0	0	0	94	86	79	0	0	0	0	0	0	0	0	0	0	0
		90	99	91	72	99	92	99	99	99	99	99	99	96	98	99	99	99	99	99	99	99	99	99	99	99	91	93	99	92	99	99	99	98	99
		89	88	92	97	96	96	99	99	99	99	99	99	99	99	99	99	99	99	97	99	99	98	97	98	99	91	99	99	99	98	92	99	98	98
		99	99	64	98	97	98	99	87	99	99	98	98	99	98	99	99	99	98	99	97	99	99	98	95	99	99	97	95	96	99	99	98	99	98
		0	47	22	42	51	50	52	55	48	49	51	39	52	52	99	99	40	0	67	93	88	72	89	98	0	0	0	0	0	0	0	0	0	0
		0	0	0	0	0	0	0	0	0	0	0	0	0	0	0	0	0	0	0	0	0	0	0	99	99	94	96	99	98	99	98	92	98	99

Figure A1. *Observation sites included in the ozone reanalyses used in RA_LONG (1990-2013: red), RA_ALL (1990-2013, red+yellow) and RA_TOT (1990-2023; red+yellow+blue). Annual capture of hourly observations is given as a number (%). Sites that are considered as interchangeable are not separated by horizontal line (SE02 and SE14, NO01 and NO02, NO489 and NO56). For geographical location of sites, see Figure 1.*

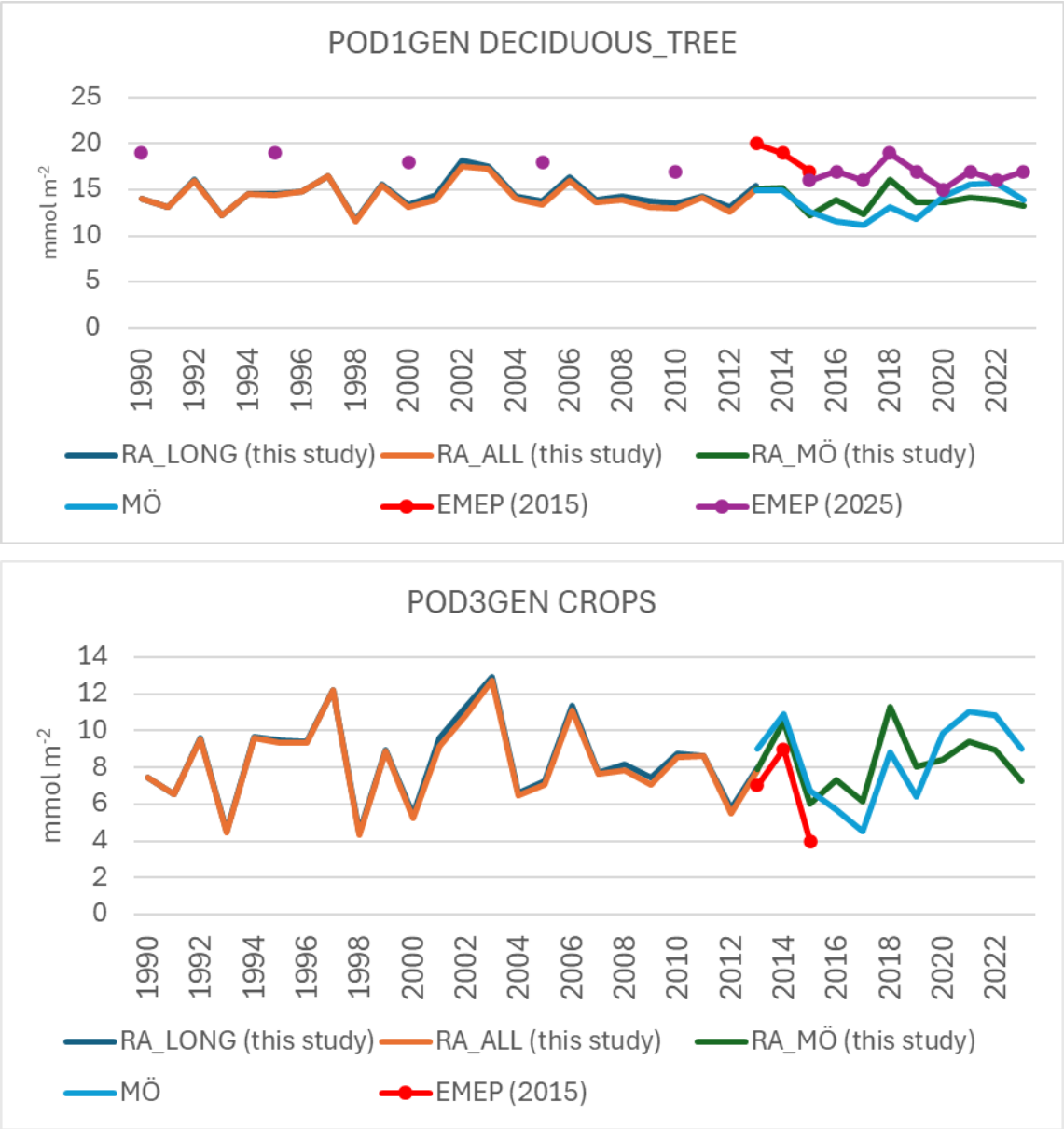

Figure A2. *Annual variation of PODY, 1990 through 2023, for generic deciduous tree (top) and generic crops (bottom). Data averaged over all Swedish land. Results from different setups in the present study are compared with results from EMEP. Note the overlap in 2013 (and in 2015 for the two EMEP data sets of generic deciduous tree). EMEP (2015) and EMEP (2025) are extracted from Gauss et al. (2015) and Klein et al. (2025), respectively.*

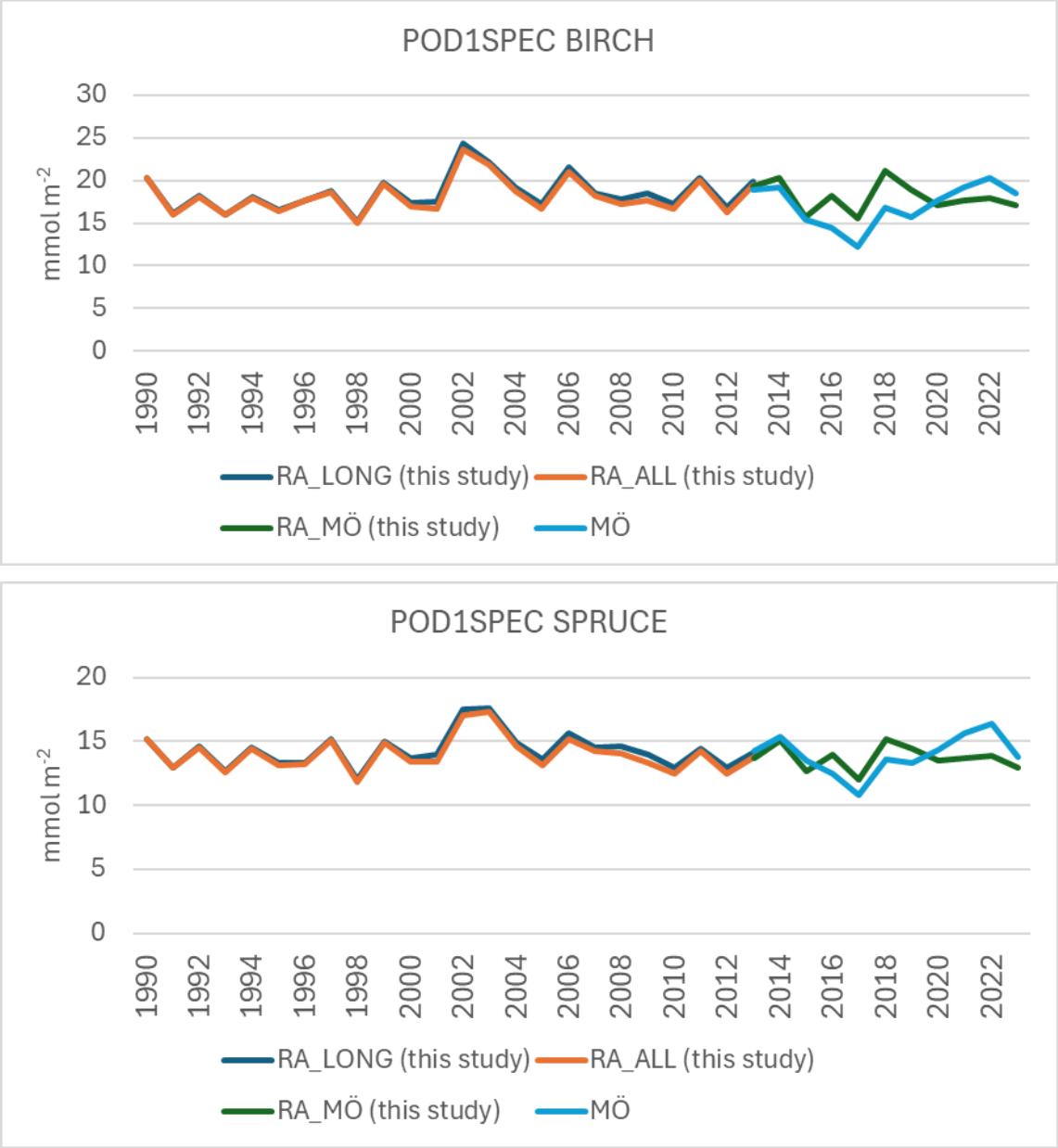

Figure A3. *Annual variation of POD1spec, 1990 through 2023, for Birch (top) and Spruce (bottom). Data averaged over all Swedish land. Results from different setups in the present study. Note the overlap in 2013.*

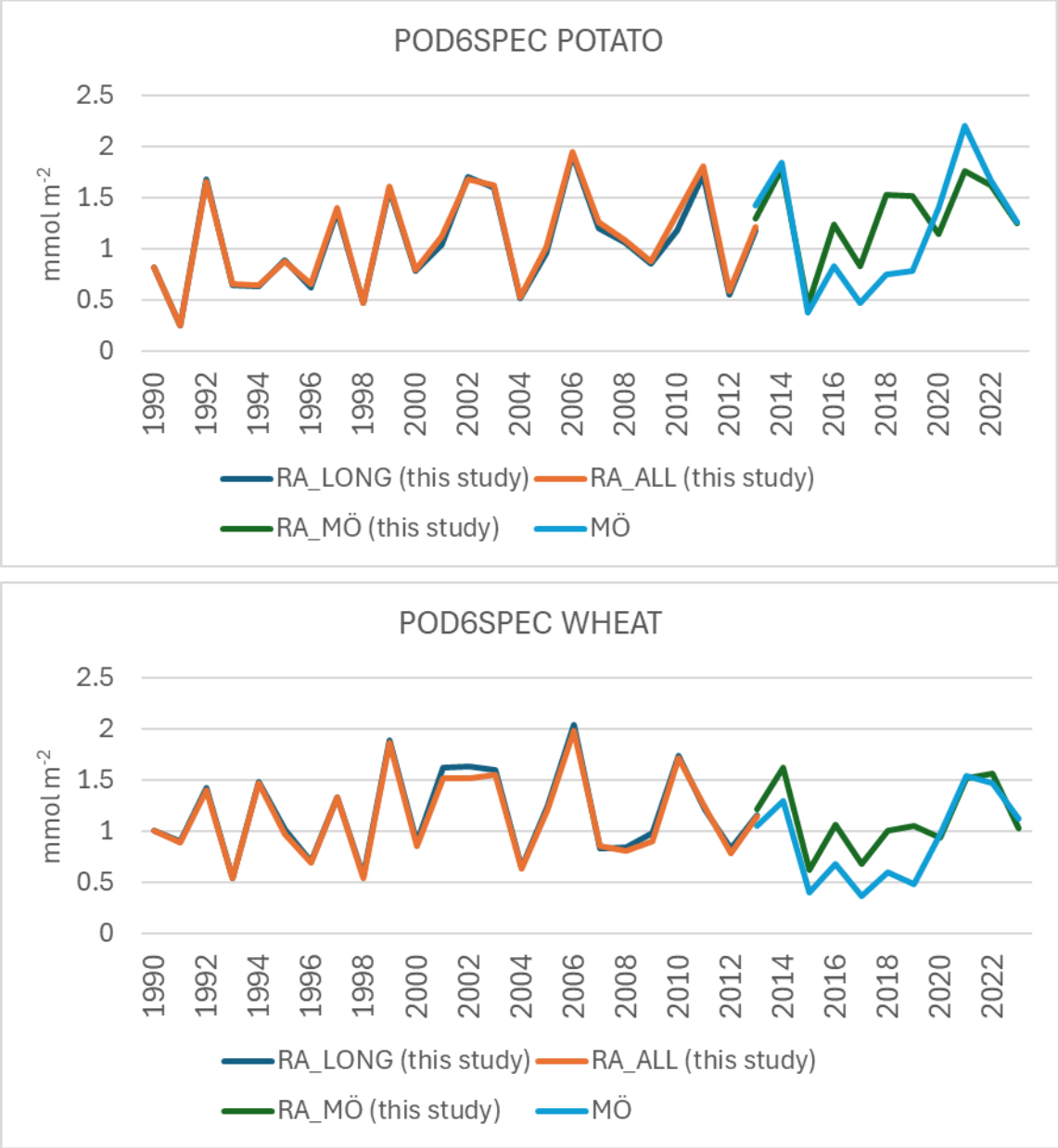

Figure A4. *Annual variation of POD6spec, 1990 through 2023, for Potato (top) and Wheat (bottom). Data averaged over all Swedish land. Results from different setups in the present study. Note the overlap in 2013.*

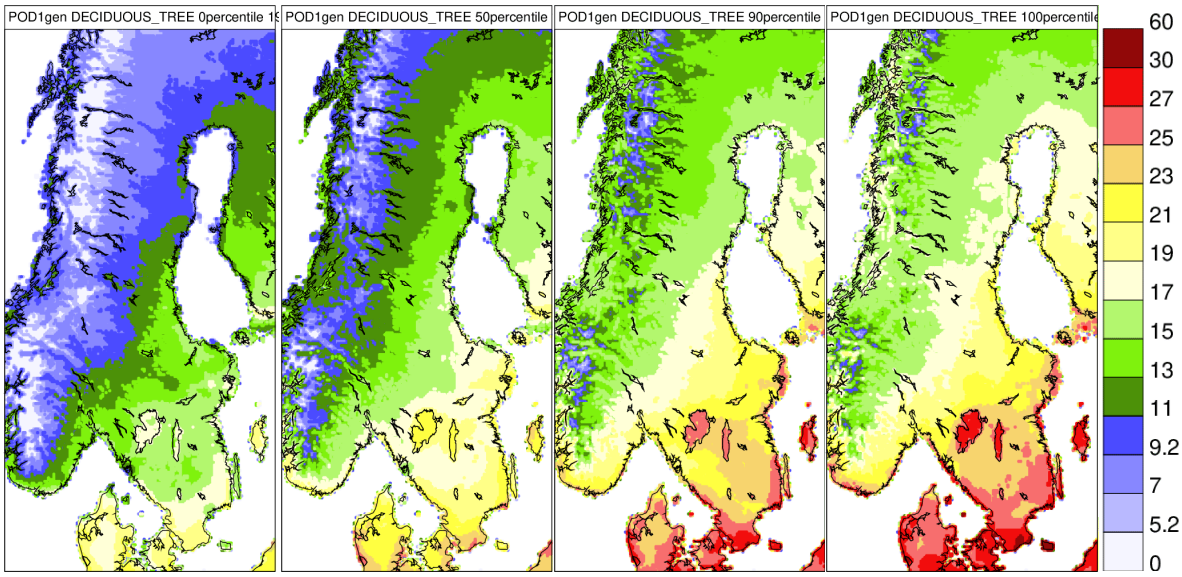

Figure A5. *Long-term percentiles of annually accumulated POD1gen deciduous tree (1990-2023). From left to right: percentiles 0 (minimum), 50 (median), 90 and 100 (maximum). Data are based on the reanalysis including all observations (RA_TOT). Unit: mmol m^{-2}. Note the different color scales between Figures A4-A6 and A7-A9.*

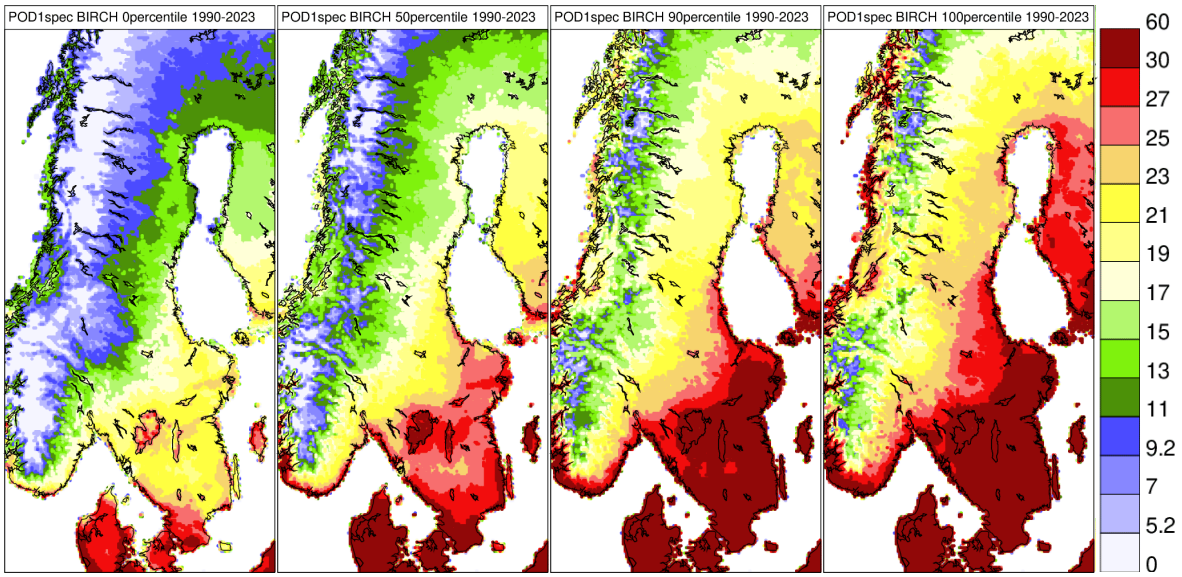

Figure A6. *Long-term percentiles of annually accumulated POD1spec birch (1990-2023). From left to right: percentiles 0 (minimum), 50 (median), 90 and 100 (maximum). Data are based on the reanalysis including all observations (RA_TOT). Unit: mmol m^{-2}. Note the different color scales between Figures A4-A6 and A7-A9.*

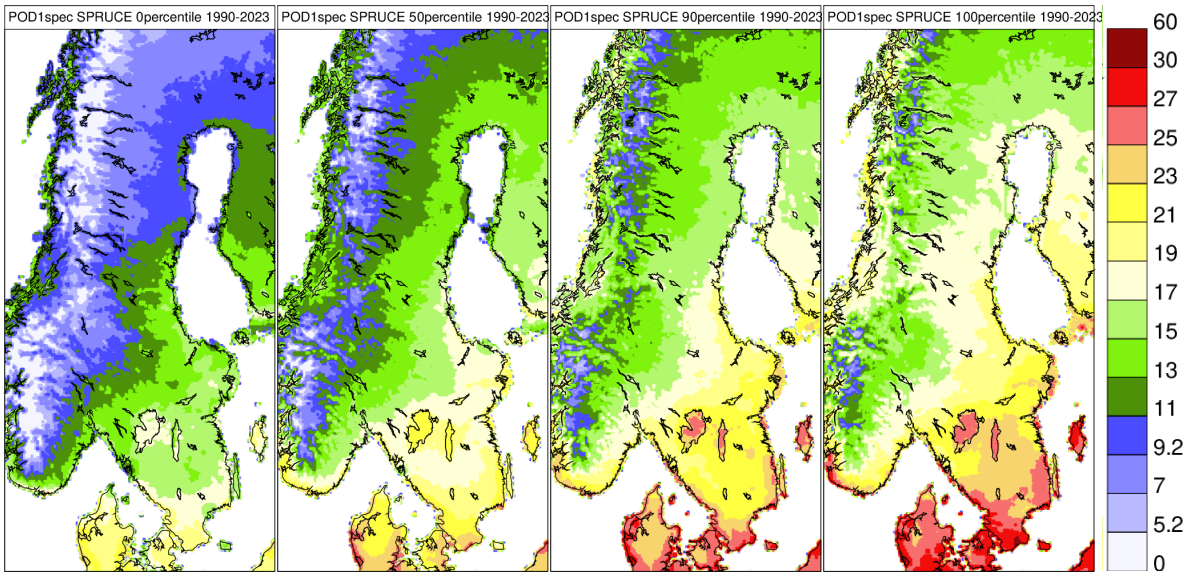

Figure A7. *Long-term percentiles of annually accumulated POD1spec spruce (1990-2023). From left to right: percentiles 0 (minimum), 50 (median), 90 and 100 (maximum). Data are based on the reanalysis including all observations (RA_TOT). Unit: mmol m^{-2}. Note the different color scales between Figures A4-A6 and A7-A9.*

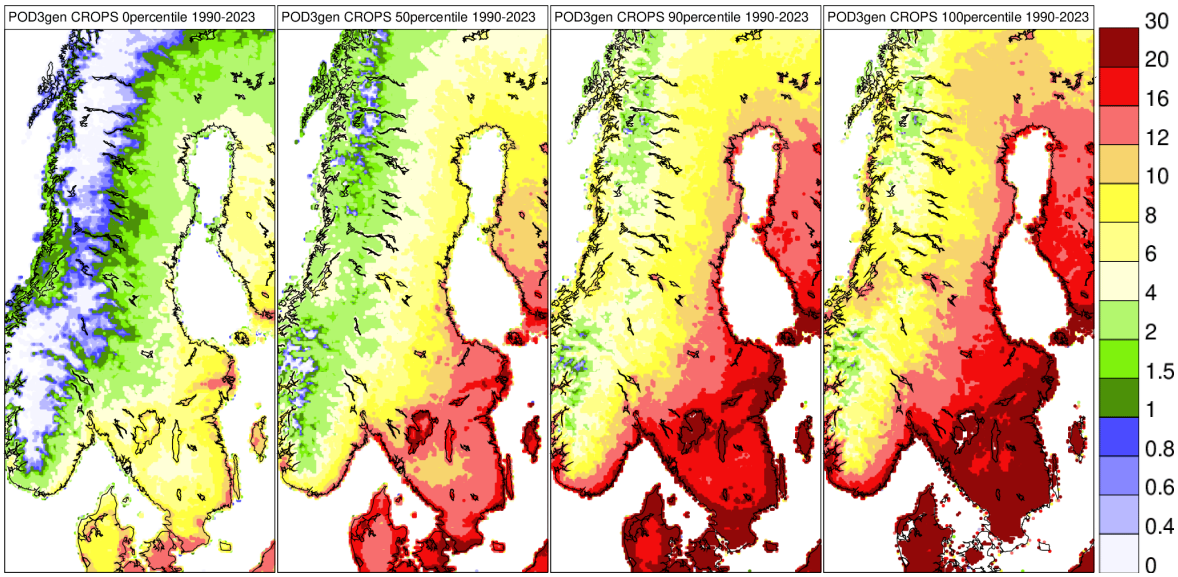

Figure A8. *Long-term percentiles of annually accumulated POD3gen crops (1990-2023). From left to right: percentiles 0 (minimum), 50 (median), 90 and 100 (maximum). Data are based on the reanalysis including all observations (RA_TOT). Unit: mmol m^{-2}. Note the different color scales between Figures A4-A6 and A7-A9.*

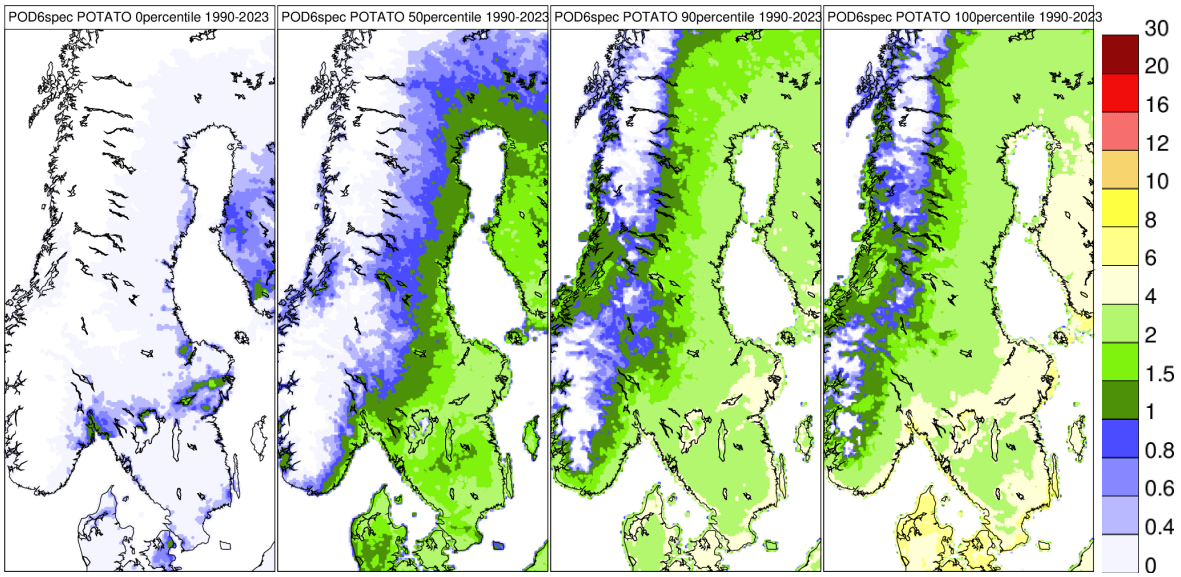

Figure A9. *Long-term percentiles of annually accumulated POD6spec potato (1990-2023). From left to right: percentiles 0 (minimum), 50 (median), 90 and 100 (maximum). Data are based on the reanalysis including all observations (RA_TOT). Unit: mmol m^{-2}. Note the different color scales between Figures A4-A6 and A7-A9.*

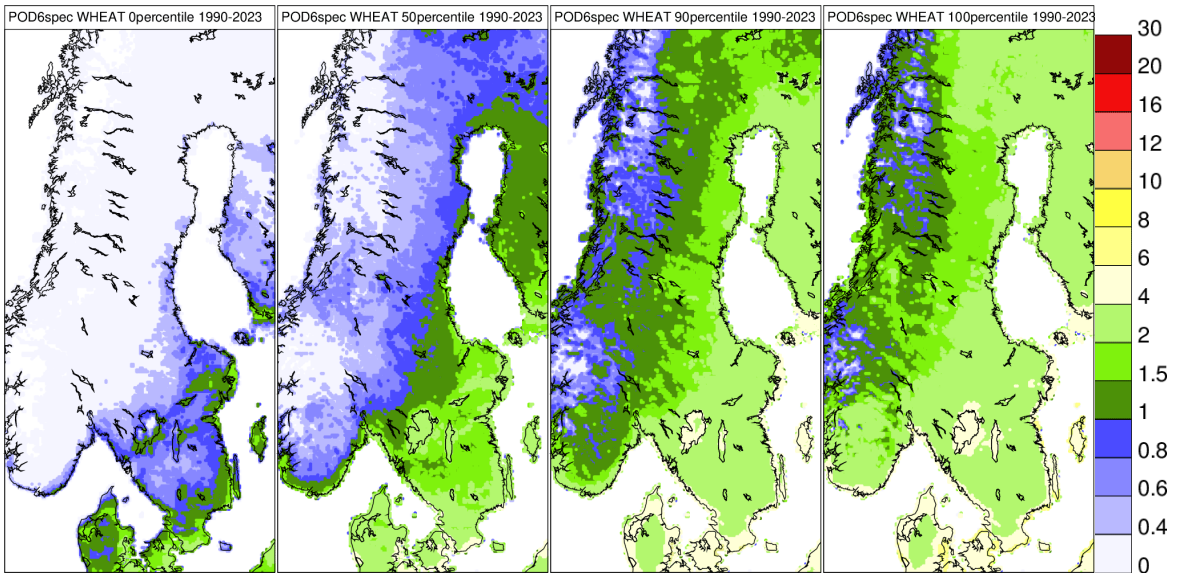

Figure A10. *Long-term percentiles of annually accumulated POD6spec potato (1990-2023). From left to right: percentiles 0 (minimum), 50 (median), 90 and 100 (maximum). Data are based on the reanalysis including all observations (RA_TOT). Unit: mmol m^{-2}. Note the different color scales between Figures A4-A6 and A7-A9.*

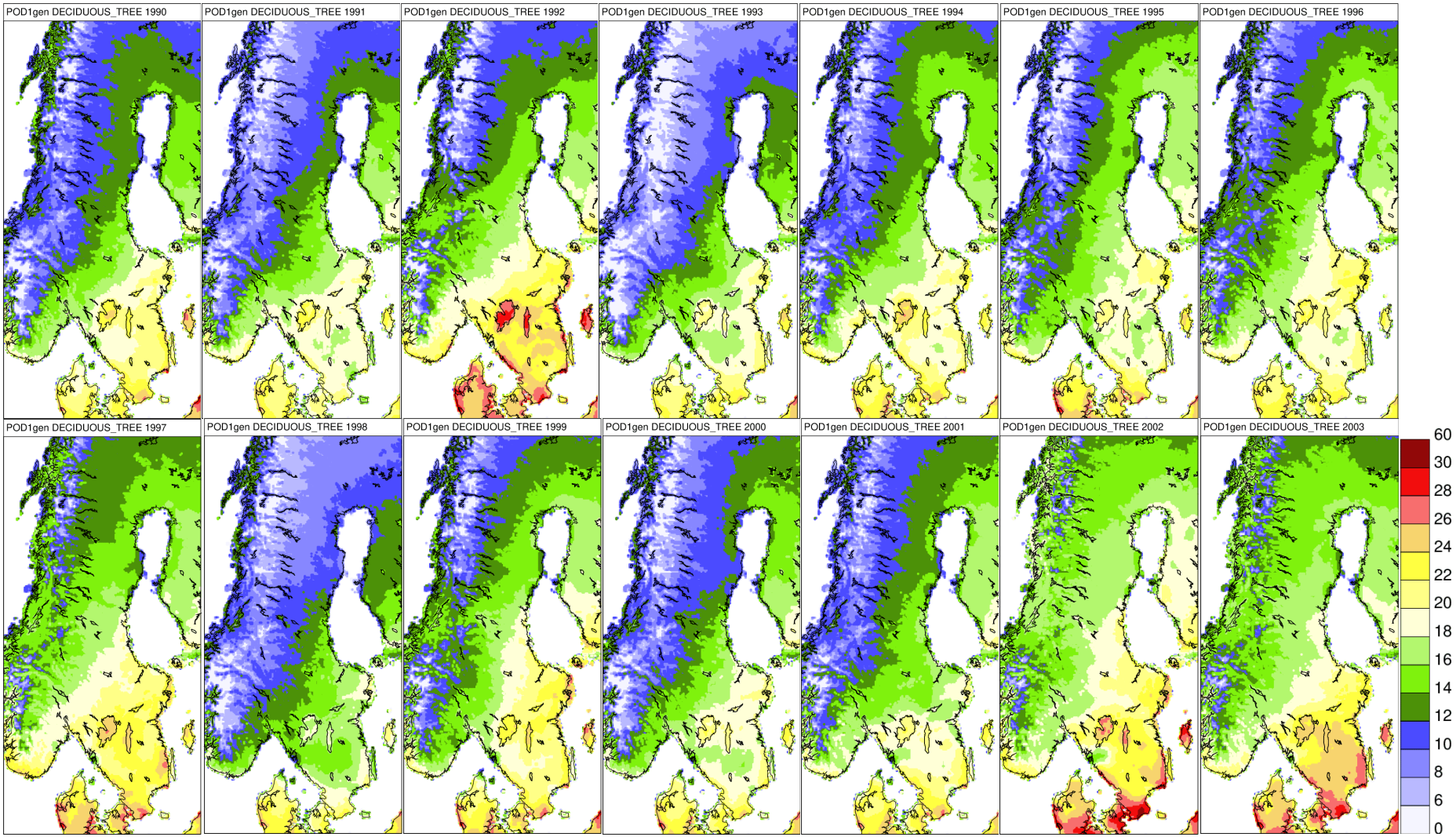

Figure A11. *Annually accumulated POD1gen deciduous trees for individual years (1990-2023). Data are based on the reanalysis including all observations (RA_TOT), but with overlap in 2013 between RA_ALL and RA_MÖ. Unit: mmol m^{-2}.*

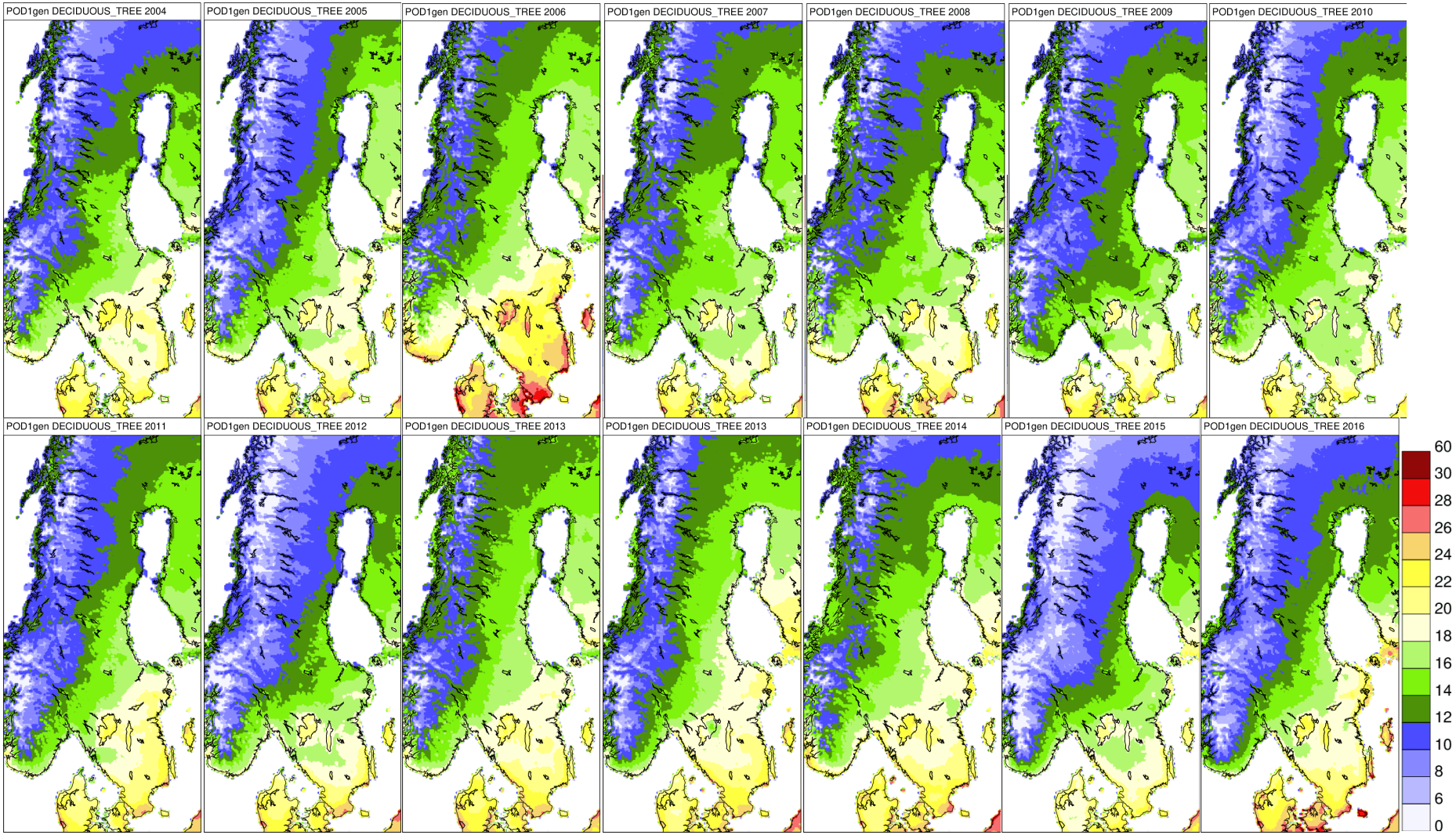

Figure A11. *Annually accumulated POD1gen deciduous trees for individual years (1990-2023), continued. Data are based on the reanalysis including all observations (RA_TOT), but with overlap in 2013 between RA_ALL and RA_MÖ. Unit: mmol m^{-2}.*

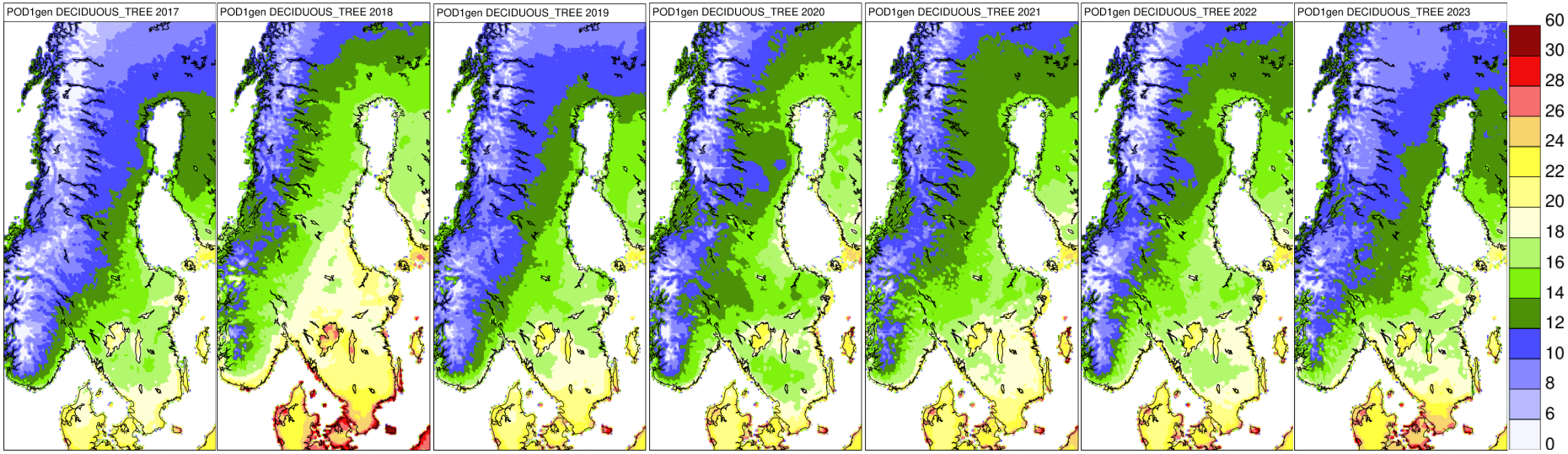

Figure A11. *Annually accumulated POD1gen deciduous trees for individual years (1990-2023), continued. Data are based on the reanalysis including all observations (RA_TOT), but with overlap in 2013 between RA_ALL and RA_MÖ. Unit: mmol m^{-2}.*

8 References

Alpfjord H. och Andersson C., 2015. Nationell miljöövervakning med MATCH Sverige-systemet - ny metodik, utvärdering och resultat för åren 2012-2013. SMHI rapport nr 2015-7. https://www.smhi.se/download/18.18f5a56618fc9f08e831d5ad/1717778942568/Slutrapport2012-13_M%C3%96_MATCH-Sverigesystemet.pdf (In Swedish)

Alpfjord Wylde, H., Leung, W. and Andersson, C. (2023). Nationell miljöövervakning med MATCH Sverigesystemet - utvärdering och resultat för åren 2019-2021. SMHI rapport Nr 2023-34. https://www.smhi.se/download/18.18f5a56618fc9f08e831d5a9/1717778941696/Slutrapport_2019-2021_MATCH-Sverigesystemet.pdf (In Swedish)

Andersson, C., Engardt, M. and Alpfjord, H, 2015. Återanalys av marknära ozon i Sverige för perioden 1990-2013. SMHI Rapport Nr 2015-80. (In Swedish)

Andersson, C., Alpfjord, H., Robertson, L., Karlsson, P. E. and Engardt, M. 2017. Reanalysis of and attribution to near-surface ozone concentrations in Sweden during 1990–2013. Atmos. Chem. Phys. 17, 13869-13890. https://doi.org/10.5194/acp-17-13869-2017

Andersson, C. and Langner, J. 2023. Utvärdering av POD1 för gran- och björkskog i MATCH Sverigesystemet. SMHI Rapport nr 2023-08.

Andersson, C., Olenius, T., Alpfjord Wylde, H., Almroth-Rosell, E., Björk, R.G., Björkman, M.P., Moldan, F. and Engardt, M. 2025. Long-term reanalysis, future scenarios and impacts of nitrogen deposition on northern European ecosystems including the Baltic Sea and the Scandinavian mountains. Science of the Total Environment 972, 179083. https://doi.org/10.1016/j.scitotenv.2025.179083

Bergström, R. and Olenius, T. 2025. Atmospheric Ammonia in Sweden: Regional Modeling and Assessment of National Emission Reduction Benefits. Tellus B: Chemical and Physical Meteorology, 77(1): 59–74. https://doi.org/10.16993/tellusb.1881

Engardt, M., Alpfjord, H. and Andersson, C. 2016. PODY-beräkningar med MATCH Sverigesystemet. Swedish Meteorological and Hydrological Institute, METEOROLOGI Nr 160. (In Swedish).

Gauss, M., Semeena, V.S., Benedictow, A. and Klein, H. 2015. Transboundary air pollution by main pollutants (S, N, O3) and PM in 2013. Sweden. MSC-W Data Note 1/2015.

Karlsson, P.E., Pihl Karlsson, G. and Pleijel, H. 2018. *En förbättrad metodik för att beräkna ozonkänsliga perioder för växtligheten under året*. **IVL Rapport U 6011**.

Karlsson, P.E., Danielsson, H., Pleijel, H and Andersson, C. 2024. Exceedance of critical levels for ozone impacts on Swedish forests Evaluation of methodology for POD1SPEC calculations. IVL. 70pp.

Klein, H., Gauss, M., Tsyro, S. and Nyíri, Á. 2025. Transboundary air pollution by sulphur, nitrogen, ozone and particulate matter in 2023. Sweden. MSC-W Data Note 1/2025.

Langner, J., Alpfjord Wylde, H and Andersson, C. 2019. *Mapping of phytotoxic ozone dose for birch, spruce, wheat and potato using the MATCH-Sweden System*. METEOROLOGI Nr 166.

Ridal et al. 2024. CERRA, the Copernicus European Regional Reanalysis system. *Quarterly Journal of the Royal Meteorological Society* **150**, 3385–3411.

Simpson, D., Segers, A., Valdebenito, A. and Fagerli, H. 2021. Modelling of phyto-toxic ozone doses for Norway. Norwegian Meteorological Institute. Metreport No. 16/2021. 53 pp. https://www.miljodirektoratet.no/publikasjoner/2022/mars/modelling-of-phyto-toxic-ozone-doses-for-norway/

UNECE 2024. *Final report. Manual on Methodologies and Criteria for Modelling and Mapping Critical Loads and Levels and Air Pollution Effects, Risks, and Trends. Update 2024.* German Environment Agency. **Texte 123/2024**.

Copernicus Climate Data Store (CDS): https://cds.climate.copernicus.eu/

SMHI. MATCH Sweden System data service. Available at: https://www.smhi.se/data/miljo/atmosfarskemi

9 SMHI Publications

SMHI publish seven reportseries. Three of these, the R-series, are intended for international readers and are in most cases written in English. For the others the Swedish language is used.

Name of the series	Published since
RMK (Report Meteorology and Climatology)	1974
RH (Report Hydrology)	1990
RO (Report Oceanography)	1986
METEOROLOGI	1985
HYDROLOGI	1985
OCEANOGRAFI	1985
KLIMATOLOGI	2009

SMHI Publications

SMHI publishes seven report series. Three of these, the R-series, are intended for international readers and are in most cases written in English. For the others the Swedish language is used.

Names of the Series Published since

RMK (Report Meteorology and Climatology) 1974

RH (Report Hydrology) 1990

RO (Report Oceanography) 1986

METEOROLOGI 1985

HYDROLOGI 1985

OCEANOGRAFI 1985
KLIMATOLOGI 2009

Earlier issues published in serie RMK

1 Thompson, T. Udin, I. and Omstedt, A. (1974)
Sea surface temperatures in waters surrounding Sweden

2 Bodin, S. (1974)
Development on an unsteady atmospheric boundary layer model

3 Moen, L. (1975)
A multi-level quasi-geostrophic model for short range weather predictions

4 Holmström, I. (1976)
Optimization of atmospheric models

5 Collins, W.G. (1976)
A parameterization model for calculation of vertical fluxes of momentum due to terrain induced gravity waves

6 Nyberg, A. (1976)
On transport of sulphur over the North Atlantic

7 Lundqvist, J-E. Udin, I. (1977)
Ice accretion on ships with special emphasis on Baltic conditions

8 Eriksson, B. (1977)
Den dagliga och årliga variationen av temperatur, fuktighet och vindhastighet vid några orter i Sverige

9 Holmström, I. and Stokes, J. (1978)
Statistical forecasting of sea level changes in the Baltic

10 Omstedt, A. and Sahlberg, J. (1978)
Some results from a joint Swedish-Finnish sea ice experiment, March, 1977

11 Haag, T. (1978)
Byggnadsindustrins väderberoende, seminarieuppsats i företagsekonomi, B-nivå

12 Eriksson, B. (1978)
Vegetationsperioden i Sverige beräknad från temperaturobservationer

13 Bodin, S. (1979)
En numerisk prognosmodell för det atmosfäriska gränsskiktet, grundad på den turbulenta energiekvationen

14 Eriksson, B. (1979)
Temperaturfluktuationer under senaste 100 åren

15 Udin, I. och Mattisson, I. (1979)
Havsis- och snöinformation ur datorbearbetade satellitdata - en modellstudie

16 Eriksson, B. (1979)
Statistisk analys av nederbördsdata. Del I. Arealnederbörd

17 Eriksson, B. (1980)
Statistisk analys av nederbördsdata. Del II. Frekvensanalys av månadsnederbörd

18 Eriksson, B. (1980)
Årsmedelvärden (1931-60) av nederbörd, avdunstning och avrinning

19 Omstedt, A. (1980)
A sensitivity analysis of steady, free floating ice

20 Persson, C. och Omstedt, G. (1980)
En modell för beräkning av luftföroreningars spridning och deposition på mesoskala.

21 Jansson, D. (1980)
Studier av temperaturinversioner och vertikal vindskjuvning vid Sundsvall-Härnösands flygplats

22 Sahlberg, J. and Törnevik, H. (1980)
A study of large scale cooling in the Bay of Bothnia

23 Ericson, K. and Hårsmar, P.-O. (1980)
Boundary layer measurements at Klockrike Oct 1977

24 Bringfelt, B. (1980)
A comparison of forest evapotranspiration determined by some independent methods

25 Bodin, S. and Fredriksson, U. (1980)
Uncertainty in wind forecasting for wind power networks

26 Eriksson, B. (1980)
Graddagsstatistik för Sverige

27 Eriksson, B.(1981)
Statistisk analys av nederbördsdata. Del III. 200-åriga nederbördsserier

28 Eriksson, B. (1981)
Den "potentiella" evapotranspirationen i Sverige

29 Pershagen, H. (1981)
Maximisnödjup i Sverige (perioden 1905-70)

30 Lönnqvist, O. (1981)
Nederbördsstatistik med praktiska tillämpningar
(Precipitation statistics with practical applications.)

31 Melgarejo, J.W. (1981)
Similarity theory and resistance laws for the atmospheric boundary layer

32 Liljas, E. (1981)
Analys av moln och nederbörd genom automatisk klassning av AVHRR-data

33 Ericson, K. (1982)
Atmospheric boundary layer field experiment in Sweden 1980, GOTEX II, part I

34 Schoeffler, P. (1982)
Dissipation, dispersion and stability of numerical schemes for advection and diffusion

35 Undén, P. (1982)
The Swedish Limited Area Model. Part A. Formulation

36 Bringfelt, B. (1982)
A forest evapotranspiration model using synoptic data

37 Omstedt, G. (1982)
Spridning av luftförorening från skorsten i konvektiva gränsskikt

38 Törnevik, H. (1982)
An aerobiological model for operational forecasts of pollen concentration in the air

39 Eriksson, B. (1982)
Data rörande Sveriges temperaturklimat.

40 Omstedt, G. (1984)
An operational air pollution model using routine meteorological data

41 Persson, C. and Funkquist, L. (1984)
Local scale plume model for nitrogen
oxides. Model description

42 Gollvik, S. (1984)
Estimation of orographic precipitation by dynamical interpretation of synoptic model data

43 Lönnqvist, O. (1984)
Congression - A fast regression technique with a great number of functions of all predictors

44 Laurin, S. (1984)
Population exposure to SO and NO_x from different sources in Stockholm

45 Svensson, J. (1985)
Remote sensing of atmospheric temperature profiles by TIROS Operational Vertical Sounder

46 Eriksson, B. (1986)
Nederbörds- och humiditetsklimat i Sverige under vegetationsperioden

47 Taesler, R. (1986)
Köldperioden av olika längd och förekomst

48 Wu Zengmao (1986)
Numerical study of lake-land breeze over Lake Vättern, Sweden

49 Wu Zengmao (1986)
Numerical analysis of initialization procedure in a two-dimensional lake breeze model

50 Persson, C. (1986)
Local scale plume model for nitrogen oxides. Verification

51 Melgarejo, J.W. (1986)
An analytical model of the boundary layer above sloping terrain with an application to observations in Antarctica

52 Bringfelt, B. (1986)
Test of a forest evapotranspiration model

53 Josefsson, W. (1986)
Solar ultraviolet radiation in Sweden

54 Dahlström, B. (1986)
Determination of areal precipitation for the Baltic Sea

55 Persson, C. Rodhe, H. and De Geer, L-E. (1986)
The Chernobyl accident - A meteorological analysis of how radionucleides reached Sweden

56 Persson, C. Robertson, L. Grennfelt, P. Kindbom, K. Lövblad, G. Svanberg, P.-A. (1987)
Luftföroreningsepisoden över södra Sverige 2 - 4 februari 1987

57 Omstedt, G. (1988)
An operational air pollution model

58 Alexandersson, H. and Eriksson, B. (1989)
Climate fluctuations in Sweden
1860 - 1987

59 Eriksson, B. (1989)
Snödjupsförhållanden i Sverige - Säsongerna 1950/51 - 1979/80

60 Omstedt, G. and Szegö, J. (1990)
Människors exponering för luftföroreningar

61 Mueller, L. Robertson, L. Andersson, E. and Gustafsson, N. (1990)
Mesoscale objective analysis of near surface temperature, humidity and wind. And its application in air pollution modelling

62 Andersson, T. and Mattisson, I. (1991)
A field test of thermometer screens

63 Alexandersson, H. Gollvik, S. and Meuller, L. (1991)
An energy balance model for prediction of surface temperatures

64 Alexandersson, H. and Dahlström, B. (1992)
Future climate in the Nordic region -
survey and synthesis for the next century

65 Persson, C. Langner, J. and Robertson, L. (1994)
Regional spridningsmodell för Göteborgs och Bohus, Hallands och Älvsborgs län.
A mesoscale air pollution dispersion model for the Swedish west-coast region
(In Swedish with captions also in English)

66 Karlsson, K.-G. (1994)
Satellite-estimated cloudiness from NOAA AVHRR data in the Nordic area during 1993

67 Karlsson, K-G. (1996)
Cloud classifications with the SCANDIA model

68 Persson, C. and Ullerstig, A. (1996)
Model calculations of dispersion of lindane over Europe. Pilot study with comparisons to measurements around the Baltic Sea and the Kattegatt

69 Langner, J. Persson, C. Robertson, L. and Ullerstig, A. (1996)
Air pollution Assessment Study Using the MATCH Modelling System. Application to sulphur and nitrogen compounds over Sweden 1994

70 Robertson, L. Langner, J. and Engardt, M.
(1996)
MATCH - Meso-scale Atmospheric Transport and Chemistry modelling system

71 Josefsson, W. (1996)
Five years of solar UV-radiation monitoring in Sweden

72 Persson, C. Ullerstig, A. Robertson, L. Kindbom, K. and Sjöberg, K. (1996)
The Swedish Precipitation Chemistry Network. Studies in network design using the MATCH modelling system and statistical methods

73 Robertson, L. (1996)
Modelling of anthropogenic sulphur deposition to the African and South American continents

74 Josefsson, W. (1996)
Solar UV-radiation monitoring 1996

75 Häggmark, L. Ivarsson, K.-I. Olofsson, P.-O. (1997)
MESAN - Mesoskalig analys

76 Bringfelt, B. Backström, H. Kindell, S. Omstedt, G. Persson, C. and Ullerstig, A. (1997)
Calculations of PM-10 concentrations in Swedish cities- Modelling of inhalable particles

77 Gollvik, S. (1997)
The Teleflood project, estimation of precipitation over drainage basins

78 Persson, C. and Ullerstig, A. (1997)
Regional luftmiljöanalys för Västmanlands län baserad på MATCH modell-beräkningar och mätdata - Analys av 1994 års data

79 Josefsson, W. and Karlsson, J.-E. (1997)
Measurements of total ozone 1994-1996

80 Rummukainen, M. (1997)
Methods for statistical downscaling of GCM simulations

81 Persson, T. (1997)
Solar irradiance modelling using satellite retrieved cloudiness - A pilot study

82 Langner, J. Bergström, R. and Pleijel, K. (1998)
European scale modelling of sulfur, oxidized nitrogen and photochemical oxidants. Model development and evaluation for the 1994 growing season

83 Rummukainen, M. Räisänen, J. Ullerstig, A. Bringfelt, B. Hansson, U. Graham, P. and Willén, U. (1998)
RCA - Rossby Centre regional Atmospheric climate model: model

description and results from the first multi-year simulation

84 Räisänen, J. and Doescher, R. (1998)
Simulation of present-day climate in Northern Europe in the HadCM2 OAGCM

85 Räisänen, J. Rummukainen, M. Ullerstig, A. Bringfelt, B. Hansson, U. and Willén. U. (1999)
The First Rossby Centre Regional Climate Scenario - Dynamical Downscaling of CO_2-induced Climate Change in the HadCM2 GCM

86 Rummukainen, M. (1999)
On the Climate Change debate

87 Räisänen, J. (2000)
CO_2-induced climate change in northern Europe: comparison of 12 CMIP2 experiments

88 Engardt, M. (2000)
Sulphur simulations for East Asia using the MATCH model with meteorological data from ECMWF

89 Persson, T. (2000)
Measurements of Solar Radiation in Sweden 1983-1998

90 Michelson, D. B. Andersson, T. Koistinen, J. Collier, C. G. Riedl, J. Szturc, J. Gjertsen, U. Nielsen, A. and Overgaard, S. (2000)
BALTEX Radar Data Centre Products and their Methodologies

91 Josefsson, W. (2000)
Measurements of total ozone 1997 – 1999

92 Andersson, T. (2000)
Boundary clear air echoes in southern Sweden

93 Andersson, T. (2000)
Using the Sun to check some weather radar parameters

94 Rummukainen, M. Bergström, S. Källén, E. Moen, L. Rodhe, J. and Tjernström, M. (2000)
SWECLIM – The First Three Years

95 Meier, H. E. M. (2001)
The first Rossby Centre regional climate scenario for the Baltic Sea using a 3D coupled ice-ocean model

96 Landelius, T. Josefsson, W. and Persson, T. (2001)
A system for modelling solar radiation parameters with mesoscale spatial resolution

97 Karlsson, K.-G. (2001)
A NOAA AVHRR cloud climatology over Scandinavia covering the period 1991-2000

98 Bringfelt, B. Räisänen, J. Gollvik, S. Lindström, G. Graham, P. and Ullerstig, A. (2001)
The land surface treatment for the Rossby Centre Regional Atmospheric Climate Model - version 2 (RCA2)

99 Kauker, F. and Meier, H E M. (2002)
Reconstructing atmospheric surface data for the period 1902-1998 to force a coupled
ocean-sea ice model of the Baltic Sea

100 Klein, T. Bergström, R. and Persson, C. (2002)
Parameterization of dry deposition in MATCH

101 Räisänen, J. Hansson, U. Ullerstig A. Doescher, R. Graham, L. P. Jones, C. Meier, M. Samuelsson, P. and Willén, U. (2003)
GCM driven simulations of recent and future climate with the Rossby Centre coupled atmosphere - Baltic Sea regional climate model RCAO

102 Tjernström, M. Rummukainen, M. Bergström, S. Rodhe, J. and Persson, G. (2003)
Klimatmodellering och klimatscenarier ur SWECLIMs perspektiv

103 Segersson, D. (2003)
Numerical Quantification of Driving Rain on Buildings

104 Rummukainen, M. and the SWECLIM participants (2003)
The Swedish regional climate modelling program 1996-2003 Final report

105 Robertson, L. (2004)
Extended back-trajectories by means of adjoint equations

106 Rummukainen, M. Bergström S. Persson G. Ressner, E. (2005)
Anpassningar till klimatförändringar

107 Will not be published

108 Kjellström, E. Bärring, L. Gollvik, S. Hansson, U. Jones, C. Samuelsson, P. Rummukainen, M. Ullerstig, A. Willén, U. Wyser, K. (2005)
A 140-year simulation of European climate with the new version of the Rossby Centre regional atmospheric climate model (RCA3)

109 Meier, H.E.M. Andréasson, J. Broman, B. Graham, L. P. Kjellström, E. Persson, G. and Viehhauser, M. (2006)
Climate change scenario simulations of wind, sea level, and river discharge in the Baltic Sea and Lake Mälaren region – a dynamical downscaling approach from global to local scales

110 Wyser, K. Rummukainen, M. Strandberg, G. (2006)
Nordic regionalisation of a greenhouse-gas stabilisation scenario

111 Persson, G. Bärring, L. Kjellström, E. Strandberg G. Rummukainen, M. (2007).
Climate indices for vulnerability assessments

112 Jansson, A. Persson, Ch. Strandberg, G. (2007)2D meso-scale re-analysis of precipitation, perature and wind over Europe - ERAMESAN

113 Lind, P. Kjellström, E. (2008)
Temperature and Precipitation changes in Sweden; a wide range of model-based projections for the 21st century

114 Klein, T. Karlsson, P-E. Andersson, S. Engardt, M. Sjöberg, K. (2011)
Assessing and improving the Swedish forecast and information capabilities for ground-level ozone

115 Andersson, C. Bergström, R. Bennet, C. Thomas, M. Robertson, L. SMHI. Kokkola, H. Korhonen, H. Lehtinen, K. FMI (2013)
MATCH-SALSA Multi-scale Atmospheric Transport and Chemistry model coupled to the SALSA aerosol microphysics model

116 Strandberg, G. Bärring, L. Hansson, U. Jansson, C. Jones, C. Kjellström, E. Kolax, M. Kupiainen, M. Nikulin, G. Samuelsson, P. Ullerstig, A. and Wang, S. (2014)
CORDEX scenarios for Europe from the Rossby Centre regional climate model RCA4

117 Lennart Bengtsson, Nils Gustafsson1), Bo Döös2), Daniel Söderman, Lars Moen3), Thomas Thompson4), Paul Jakobsson, Gunnar Bleckert, Ann-Beate Henriksson, Bo Lindgren5) and Per Kållberg
1)Correspondig author, e-mail: Nils.Gustafsson@smhi.se
2)Deceased 2010 3)Deceased 2006
4)Deceased 2015 5)Deceased 2005
The Meteorological Auto Code (MAC) and Numerical Weather Prediction (NWP) at SMHI

118 Sandra Andersson, Lars Bärring, Tomas Landelius, Patrick Samuelsson, Sejmon Schimanke (2021)
SMHI Gridded Climatology

119 Helene Alpfjord Wylde, Christian Asker, Cecilia Bennet, Bertil Forsberg (Umeå University), David Segersson (2022
Quantification of population exposure to PM10, PM2.5 and NO2 and estimated health impacts for 2019 and 2030

120 Maria Grundström, Christian Asker, David Segersson, Helene Alpfjord Wylde, Eef van Dongen, Mattias Jakobsson, Fredrik Windmark (2023)
High resolution air quality modelling of NO2, PM10 and PM2.5 for Sweden A national study for 2019 based on dispersion modelling from regional down to street canyon level

121 Fredrik Windmark, Maria Grundström, Mattias Jakobsson, Christian Asker, Johan Arvelius (2025)
High resolution air quality modelling of NO2, PM10 and PM2.5 for Sweden. A national study for 2023 based on dispersion modelling from regional down to street canyon level

122. Eef van Dongen, Tim Solig, Fredrik Windmark, Maria Lagerström[2], Erik Ytreberg[2] (2025)

[2] Chalmers University of Technology
Leisure boat activities and emissions in Sweden

123. Christian Asker. Fredrik Windmark, Mattias Jakobsson, Johan Arvelius. Karolina Siegel, Bertil Forsberg[2], Johan Sommar[2] (2026)
[2] Umeå University Forsberg
Quantification of population exposure to NO2, PM2.5, PM10 and O3 and estimated health impacts for 2023 and 2030

Empty page

Swedish Meteorological and Hydrological Institute
SE 601 76 NORRKÖPING
Phone +46 11-495 80 00 Telefax +46 11-495 80 01

ISSN 0347-2116